UT GSBS Dissertations and Theses (Open Access)　　　　Graduate School of Biomedical Sciences

8-2015

YAP1 expression predicts sensitivity to dual AKT/P70S6K inhibition in ovarian and uterine malignancies

Rebecca A. Previs

Follow this and additional works at: http://digitalcommons.library.tmc.edu/utgsbs_dissertations

Part of the Neoplasms Commons

YAP1 EXPRESSION PREDICTS SENSITIVITY TO DUAL AKT AND P70S6K

INHIBITION IN OVARIAN AND UTERINE MALIGNANCIES

By

Rebecca Ann Previs, M.D.

APPROVED:

_____
Anil K. Sood, M.D.
Advisory Professor

_____
Gary E. Gallick, Ph.D.

_____
Prahlad Ram, Ph.D.

_____
Wei Hu, M.D., Ph.D.

_____
Pratip Bhattacharya, Ph.D.

APPROVED:

_____
Dean, The University of Texas
Graduate School of Biomedical Sciences at Houston

YAP1 EXPRESSION PREDICTS SENSITIVITY TO DUAL AKT AND P70S6K INHIBITION IN OVARIAN AND UTERINE MALIGNANCIES

A

Thesis

Presented to the Faculty of

The University of Texas

Health Science Center at Houston

And

The University of Texas

M.D. Anderson Cancer Center

Graduate School of Biomedical Sciences

In Partial Fulfillment

Of the Requirements

For the Degree of MASTER OF SCIENCE

By

Rebecca Ann Previs, M.D.

Houston, Texas

August, 2015

Dedication

For my family, who first showed me what it meant to live a life with grit.

Acknowledgements

"Anytime you see a turtle up on top of a fence post, you know he had some help."

-Alex Haley

I owe my spot on top of a fence post to many people. I would like to thank my family, who shaped me during my earliest years, encouraged me, pushed me to be my best, think creatively, be humble, work hard, and to always be grateful and graceful, something that continually is a work in progress.

Thank you Dr. Sood for your mentorship and giving me the opportunity to learn that I could become a physician-scientist. You have given me the tools and language to solve clinical questions in a meaningful and scientific way. Thank you for pushing me beyond what I thought I was capable of. I am grateful that you believed in me even though I never saw a band on a western blot for six months.

Thank you to my fellowship, specifically, Drs. Frumovitz, Lu, and Soliman, for finding me a home during my research years and having the wisdom to guide my early career long before I knew what I was interested in. I am grateful for the flexibility the funding from the T32 has afforded me during this time.

I would also like to acknowledge my earliest mentors, Dr. Bill Myers, and more recently, Drs. Secord and Berchuck.

I appreciate the feedback from my committee including Drs. Gallick, Hu, Bhattacharya, and Ram.

Thank you most of all to my lab cats, who from the first day of lab kindergarten patiently taught me how to pipette and understand the complex world of biology.

I am forever grateful to Guillermo, who is more than a best friend, but also a mentor. Your willingness to talk and teach science over morning coffee and answer late night calls when science questions arose are truly appreciated but speak highly of your mentorship abilities. Thank you for constantly reminding me what is most important and supporting me. You have come through for me on so many occasions, and you are the most reliable person I know. Thank you for reining me in even when I tend to do Extreme Science.

Thank you to Rajesh, who I affectionately refer to as my "science husband," who has never once refused to answer a question, check a calculation, help me with an analysis, or teach me a technique. You are a science rockstar! I am lucky to call you a teacher and friend. Of course, it takes a village of cats, so I would also like to express my sincerest gratitude to Kshipra, Arch, Mangala, Monika, Morgan, and Jie for science help, homemade Indian treats, and being wonderful friends.

Thank you also to my co-fellows, who have been research fellows with me during my first two years: Heather; Kari, Alaina, Michaela, Lauren, Janelle, Jeannie, and Jolyn. Research breakfast fuels the soul.

I owe more than I could ever repay to Heather Dalton, my lab buddy, co-fellow, and best friend. Thank you for your advice, tough love, "Rules about Life, Science and Dating," shaking me when I lose perspective, taking me shoe shopping after a bad day, and always saving a place for me on your sofa. Thank you for countless hours of figure making with the beasts without even saying a word.

Thank you to my Sood lab family for giving me a second home and a fence post.

~Becca

YAP1 EXPRESSION PREDICTS SENSITIVITY TO DUAL AKT AND P70S6K INHIBITION IN OVARIAN AND UTERINE MALIGNANCIES

Rebecca Ann Previs, M.D.

Advisory Professor: Anil K. Sood, M.D.

Abstract

Purpose: The PI3K/AKT/P70S6K pathway is an attractive therapeutic target in ovarian and uterine malignancies due to its high rate of dysregulation and key roles in tumor growth. Here, we examined the biological effects of MSC2363318A, which is a novel inhibitor of AKT1, AKT3, and P70S6K.

Experimental Design: Orthotopic murine models of ovarian and uterine cancer were utilized to study the effect of MSC2363318A on survival and regression. Moreover, *in vitro* experiments (MTT, Western blot analysis, plasmid transfection, and reverse phase protein array [RPPA]) were carried out to characterize underlying mechanisms and potential biomarkers of response.

Results: MSC2363318A decreased tumor growth and metastases in multiple murine orthotopic models of ovarian (SKOV3ip1, HeyA8, and Igrov1) and uterine (Hec1a) cancer and reduced proliferation (Ki67) and angiogenesis (CD31) indices and increased cell death (cleaved caspase-3) markers. Synergy between MSC2363318A and paclitaxel was observed *in vitro* in protected (IC50 ≥ 5 μM) cell lines. RPPA identified YAP1 as a candidate marker to predict cell lines that were most sensitive to MSC2363318A (R=0.675, p=0.0015). After establishment of a bevacizumab resistant

endothelial cell line, RF-24, we demonstrate that resensitization to bevacizumab occurs with the addition of MSC2363318A.

Conclusions: MSC2363318A has therapeutic efficacy in multiple pre-clinical models of ovarian and uterine cancer. These findings support clinical development of dual AKT/P70S6K inhibition.

Table of Contents

List of figures

List of Tables

Introduction

Epidemiology and standard of care for ovarian and uterine malignancy

Ovarian cancer remains the seventh most common malignancy worldwide and represents approximately 4% of new cancer cases diagnosed each year in women [1]. It is the eighth most common cause of cancer deaths. The estimated five year overall survival of newly diagnosed ovarian cancer depends on the stage of disease at diagnosis. Epithelial carcinoma is the most common histologic type of ovarian cancer and accounts for 90% of cases. The histologic subtypes include high grade serous, which accounts for 70-80% of cases, endometrioid, clear cell, mucinous, and low grade serous [2,3]. Due to a lack of effective screening, vague symptomology, and advanced disease presentation, patients with advanced stage IIIC and stage IV disease have an overall survival of 32.5 and 18.6%, respectively [4].

In developed countries, uterine cancer is the most common malignancy and the second most common worldwide [1]. The majority of women (68%) are diagnosed at an earlier stage when disease is confined to the uterus [5]. This is primarily due to symptoms of postmenopausal bleeding. Adenocarcinoma of the uterus is the most common histologic subtype of uterine cancer and is broadly classified into type 1 or type 2 tumors, which differ in their incidence, responsiveness to estrogen, and clinical behavior [6,7]. Type 1 tumors are low grade (grade 1 or 2), endometrioid histology, and comprise the majority of adenocarcinomas (approximately 80%). These are primarily estrogen dependent and have a favorable prognosis. In contrast, type 2 tumors consist of high grade endometrioid histology (grade 3) and non-endometrioid histologies, including serous, clear cell, squamous, undifferentiated, mucinous and

transitional cell types. These tumors are not estrogen dependent and have a more aggressive clinical course.

Staging for both diseases can be classified generally to the location of the primary disease at diagnosis and the presence of distant metastases. Generally speaking, in stage 1 disease, tumor growth is limited to the primary disease site (either the ovary or uterus). In stage 2 disease, tumor has spread to other disease sites within the pelvis for ovary or to the vagina in uterine cancer. In stage 3 disease, tumor has spread intra-abdominally outside of the pelvis and/or to the retroperitoneal lymph nodes (Figure 1). Stage 4 comprises distant metastases including parenchymal liver involvement or malignant pleural effusions [8].

Figure 1. Laparoscopic assessment of disease burden involving the bilateral ovaries and peritoneum. Photo courtesy of Alpa Nick, M.D.
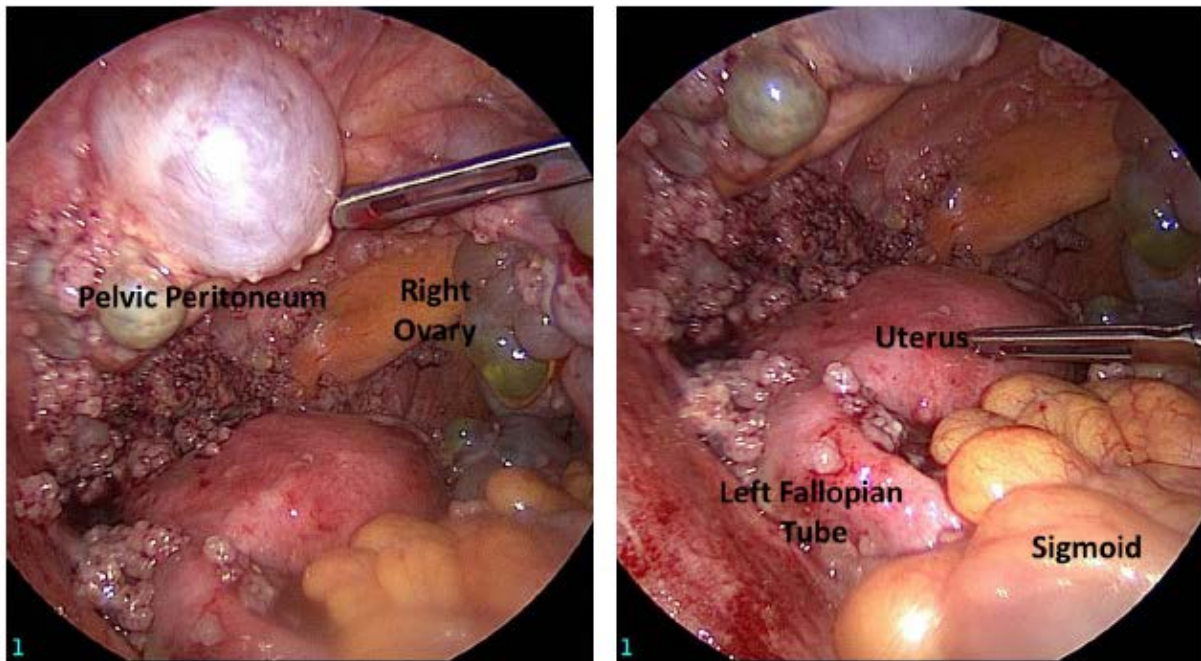
Cytroreductive surgery to no gross residual disease and comprehensive surgical staging followed by adjuvant taxane- and platinum based chemotherapy regimens

remain the mainstay of upfront treatment [9] for ovarian cancer. Despite the effectiveness of frontline treatment, the majority (62%) of women will recur and ultimately die of their disease. In women with stage III or IV disease, 80-85% will recur. Second-line chemotherapy or surgery in selected cases is offered to women with recurrent disease. More recently, anti-angiogenic therapies [10,11], PARP inhibitors in women with a BRCA mutation [12,13], and genomic testing of the tumor [14,15] have been employed to improve progression free and overall survival. Bevacizumab and olaparib were the first two biologic therapies approved for ovarian cancer.

The administration of bevacizumab as a frontline agent in women with newly diagnosed ovarian cancer has been evaluated by two randomized controlled studies: GOG218 and ICON7. In GOG218, women were randomized to receive: (1) standard chemotherapy with carboplatin and paclitaxel; (2) bevacizumab plus standard chemotherapy for six cycles followed by placebo until month 15, or (3) bevacizumab plus standard chemotherapy followed by bevacizumab until month 15. There was a significant increase in progression free survival of patients that received bevacizumab plus chemotherapy followed by bevacizumab, but there was no improvement of overall survival [16]. ICON7 randomized women newly diagnosed with ovarian cancer to standard carboplatin or paclitaxel for six cycles with or without bevacizumab during chemotherapy and then as a maintenance treatment for 12 additional cycles. While there was a significant improvement in progression free survival in the women who received bevacizumab (24 versus 22 months), there was no difference in overall survival [17].

The use of bevacizumab in the setting of relapsed disease has also been evaluated. In GOG17D, women (n=62) with platinum-resistant disease were treated with bevacizumab, and two patients had complete responses and 11 had partial responses. Median progression free survival and overall survival were 4.7 and 17 months, respectively [10]. In another Phase II study, women with platinum-resistant ovarian cancer received single agent bevacizumab and median progression free survival was 4.4 months. Median survival duration was 10.7 months [18].

In December 2014, the Food and Drug Administration granted accelerated approval for olaparib as a treatment for women with *BRCA1* or *BRCA2* mutations following three or more lines of previous chemotherapy. This approval came from Study 19, which evaluated women with BRCA-associated platinum-sensitive ovarian cancer. This trial included nearly 300 women with recurrent disease who were randomized to receive treatment with olaparib or placebo. There was a significant improvement in progression free survival (eight versus five months) in the women who were treated with olaparib [12]. An interim analysis did not show an overall survival benefit. A separate analysis of patients with a known *BRCA* mutation suggested that the clinical benefit was the highest in this subset of patients, with a significant improvement in progression free survival (11 versus 4 months) and a trend toward an improvement in overall survival [13].

Hysterectomy, bilateral salpingo-oophorectomy, with pelvic or para-aortic lymph node dissection (or sentinel lymph node assessment) is the recommended staging procedure for patients with uterine cancer [19]. In women that present with pelvic or intra-abdominal disease, complete cytoreduction has been associated with prolonged

overall survival [20]. Adjuvant treatment of women following surgery depends on their individual risk of recurrence and the presence of persistent disease. Women are stratified into low-, intermediate-, and high-intermediate, and high risk for recurrence and may receive combination taxane- and platinum based chemotherapy with or without radiation.

The estimated five year survival of newly diagnosed ovarian and uterine cancer patients can be broken down by FIGO stage. Most ovarian cancers are of epithelial origin and present with high grade and late stage; the five year overall survival is dismal, around 30%. Early stage disease uterine cancer portends a five year overall survival of 90%, but higher stage disease has five year overall survivals that are similar to that of ovary (Tables 1-2).

Table 1. Five year overall survival in ovarian cancer patients by stage at diagnosis [8].

FIGO stage	5-year Overall Survival (%)
IA	89.6
IB	86.1
IC	83.4
IIA	70.7
IIB	65.5
IIC	71.4
IIIA	46.7
IIIB	41.5
IIIC	32.5
IV	18.6

Table 2. Five year overall survival in uterine cancer patients by stage at diagnosis [19].

FIGO stage	5-year Overall Survival (%)
IA	90
IB	78
II	74
IIIA	56
IIIB	36
IIIC1	57
IIIC2	49
IVA	22
IVB	21

The Cancer Genome Atlas (TCGA) provides an important resource for understanding the molecular pathogenesis of these malignancies. Using 489 high grade serous ovarian cancer samples, TCGA analysis showed the high prevalence of *TP53* mutations in almost all of the samples (96%). Other recurrent somatic mutations were found in *NF1*, *BRCA1*, *BRCA2*, *RB1*, and *CDK12* genes [21]. Further analysis, found that homologous recombination is frequently abnormal in about half of the cases, with NOTCH and FOXM1 cell signaling also altered [21]. From the uterine cancer TCGA analysis, uterine serous tumors had frequent *TP53* mutations, extensive copy number alterations, and low levels of estrogen and progesterone receptors. In the endometrioid tumors that were examined, there were much fewer copy number

alterations and mutations in *TP53*, but there were frequent mutations in *PTEN*, *CTNNB1*, *PIK3CA*, *ARID1A*, *KRAS*, and *ARID5B.* A subset of endometrioid tumors had increased transversion mutation frequency in *POLE [22]*.

In women with recurrent, refractory disease, new therapeutic agents are needed to impact survival and potentially cure women of metastases. Multiple classes of targeted therapies have been developed to target the tumor cells in these solid malignancies and the cells within the tumor microenvironment. Within the microenvironment, targeting the vasculature with anti-vascular endothelial growth factor (VEGF) therapy with a commonly used monoclonal antibody, bevacizumab, has shown to induce partial responses and/or stable disease [10]. Bevacizumab binds VEGF, preventing it from binding to VEGF receptors. Because of the poor prognosis of ovarian and type 2 endometrial cancers with little improvement in the outcomes of women with standard surgery and adjuvant chemotherapy, a better understanding of the complex interplay of the tumor microenvironment with aberrant tumor cell signaling is warranted.

The PI3K/AKT/mTOR pathway and malignancy

The PI3K/AKT/mTOR pathway controls important cellular processes necessary for tumorigenesis and metastasis including survival, proliferation, metabolism, regulation of cell cycle, angiogenesis, and genomic instability (Figure 2) [23]. This pathway plays a pivotal role in many malignant features involved in tumor pathogenesis and is intimately linked with most of the hallmarks of cancer [24]. Genomic studies

suggest that aberrations within this signaling pathway are among the most frequently altered in malignancies.

Figure 2. Overview of the PI3K/AKT/mTOR pathway.
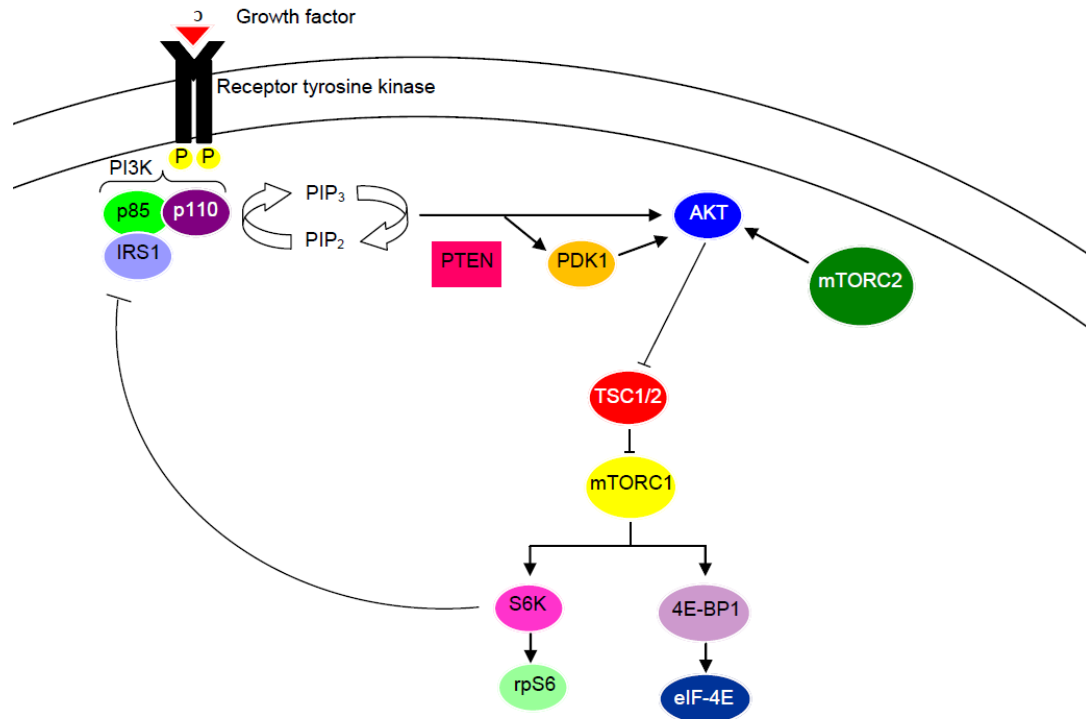
PI3K is a major downstream effector of G-coupled protein receptors and tyrosine kinase receptors. Three classes of PI3K have been recognized: (1) Class IA PI3K includes IA PIK3α, β, and δ, all of which are activated by receptors that have receptor tyrosine kinase activity; (2) Class IB PI3K includes PI3Kγ, which are subsequently activated by G-coupled protein receptors. The Class IA PI3Ks are heterodimers and consist of p110 catalytic and p85 regulatory subunits. The three genes, PIK3CA, PIK3CB, and PIK3CD, encode the three classes of 1A p110 isoforms (α, β, and δ). Of these three genes, only PIK3CA is mutated frequently in human malignancies [23].

Activated PI3K phosphorylates phosphatidylinositol 4,5-bisphosphate (PI(4,5)P2; PIP2) to generate phosphatidylinositol (3,4,5)-triphosphate (PI(3,4,5)P3; PIP3). AKT is

recruited to the cell's plasma membrane where it can be phosphorylated at its serine473 or threonine308 residues. The tumor suppressor, PTEN, and INPP4B are responsible for the negative regulation of activation. PTEN dephosphorylates PIP3 at the 3-position phosphate of PIP3, which produces PIP2. INPP4B is responsible for the dephosphorylation of phosphatidylinositol (3,4)-bisphosphate (PI(3,4)P2) to form PI(3)P at the 4-position phosphate group [25]. Constitutive activation of AKT results from the loss of either PTEN or INPP4B, which them leads to the accumulation of PIP3 or PI(3,4)P2, respectively. Phosphorylated or activated AKT phosphorylates mTOR at the serine2448 residue, which activates mTORC1. Indirectly, AKT can also active mTORC1 through phosphorylation of the tuberous sclerosis complex (TSC2). Phosphorylated TSC2 leads to the inactivation of the functional TSC1/TSC2 complex. However, when this complex is activated, TSC2 enables the conversion of Rheb-GTP (Ras homolog enriched in brain-GTP) to Ras-GDP, which then inactivates mTORC1. Once TSC2 is phosphorylated or inactivated by AKT, Rheb-GTP is responsible for stimulating the activity of mTORC1. The other complex, mTORC2, is activated through an unclear mechanism, but PI3K may be responsible for its activation [26]. Once activated, mTORC2 phosphorylates other kinases, such as AKT, kinases present in the serum and glucocorticoid, and kinases that regulate lipogenesis, the metabolism of glucose, influence apoptosis, and are involved in the cellular cytoskeleton.

Once phosphorylated, mTORC1 phosphorylates ribosomal S6 kinase-1, which regulates protein translation and 4EBP-1, the eukaryotic translation initiation factor. S6K-1 activation then leads to downstream translation of mRNA encoding ribosomal

proteins, factors responsible for elongation, and proteins responsible for cell cycle progression [27].

PI3K/AKT pathway alterations in ovarian and uterine cancer

Genetic and/or epigenetic changes lead to activation of the PI3K/AKT signaling pathway in multiple cancers. Ovarian, type 1, and type 2 uterine cancers exhibit alterations in this pathway [21,28]. Additionally, previous analyses have found this pathway to be activated in half of high grade serous ovarian carcinomas. The *PIK3CA* gene, which encodes the catalytic isoform p100α, is a commonly mutated oncogene, affecting over 30% of solid tumors [29]. *PTEN*, which encodes phosphatase and tensin homolog, is one of the most frequently mutated tumor suppressor genes and is frequently suppressed or downregulated leading to activation of the PI3K/AKT signaling pathway [30]. Frequent aberrations of this pathway in ovarian cancer include mutations in *PTEN* [31] or hypermethylation of the promoter [32], loss of heterozygosity at the INPP4B locus [25], somatic mutations in mTOR and AKT1 [33], amplification of AKT2 [34], somatic activating mutations in the *PIK3CA* gene [35], and activating mutations in the *PIK3R1* gene [36].

Uterine cancers harbor the highest rates of PI3K/AKT pathway alterations [37]. *PTEN* mutations, often occur early in uterine cancer pathogenesis, are frequently identified in type 1 tumors, and have been identified in 34-55% of endometrial cancers [22]. Other frequently identified pathway mutations in uterine cancer include *PIK3CA* (25-40%), *PIK3R1* (15-25%), and less commonly, *AKT1-3* mutations (2-5%) [38,39,40,41].

The tumor microenvironment and the PI3K/AKT pathway

Almost all cells within the tumor microenvironment are influenced by the PI3K/AKT signaling pathway. Tumor cells secrete pro-angiogenic factors including VEGF that activate quiescent endothelial cells. New vasculature originates from existing blood vessels from proliferation and activated endothelial cells through vessel co-option [42]. Additionally, cells derived from the bone marrow including monocytes, endothelial progenitor cells, and mast cells also promote the new growth and maintenance of blood vessels [43]. The PI3Ks have been established as controls of hypoxia-inducible factor (HIF)-1α expression and VEGF secretion [44,45,46]. Within the endothelial cells, the PI3Ks are responsible for the transduction of signals that are downstream of angiogenic receptors. These include receptors in the VEGF family such as VEGFR-1/Flt-1, VEGFR-2/Flk-1, and VEGFR3 [47,48,49]. Upon phosphorylation of AKT, downstream effects are activated including migration of endothelial cells, proliferation, and tubulogenesis. Additionally, other endothelial cell stimuli and ligands have been shown to activate the endothelial cell including angiopoietin-1, insulin, insulin-like growth factor-1, hepatocyte growth factor, estrogen, fluid shear stress, reactive oxygen species, and corticosteroids [50,51,52,53,54,55,56,57]. The activation of AKT by VEGF within endothelial cells requires matrix attachment and promotes endothelial cell viability [58].

Targeting the cell microenvironment, specifically the PI3K/AKT pathway, within endothelial cells, may provide a rational approach to overcoming resistance to anti-angiogenic therapy in the clinical setting.

The high prevalence of these molecular alterations in ovarian and uterine cancers, combined with the druggability of the PI3K/AKT pathway in the tumor cells and the microenvironment, represents an important therapeutic opportunity.

Hypothesis and specific aims:

Hypothesis: Dual inhibition of AKT and P70S6K will reduce tumor growth by decreasing angiogenesis, inhibiting tumor cell proliferation, and promoting apoptosis in ovarian and uterine cancer cells.

- Specific Aim 1: To determine the prevalence of PI3K/AKT/P70S6 alterations in ovarian and uterine cancer.

- Specific Aim 2: To assess the efficacy of an AKT/P70S6 inhibitor (MSC2363318A) in combination with chemotherapeutic agents (taxanes and bevacizumab) *in vitro* and *in vivo* using well-established mouse models of ovarian carcinoma.

- Specific Aim 3: To determine the mechanisms underlying the biological responses to MSC2363318A-based therapy.

Materials and Methods

Cell line maintenance and siRNA transfections

All cell lines were maintained in 5% CO_2 at 37 °C. Ovarian cancer (A2780, ES2, HeyA8, Igrov1, Ovcar3, Ovcar4, Ovcar5, Ovcar8, Ovca432, and SKOV3ip1), uterine cancer (AN3CA, Hec1A, Hec1B, Hec265, Ishikawa, KLE, RL95-2, Spec2 SKUT2, RL95-2 and KLE), and endothelial (RF-24) cells were obtained from the American Type Culture Collection. A2780, ES2, HeyA8, Igrov1, Ovcar3, Ovcar4, Ovcar8, Ovca432, SKOV3ip1, and Hec265 were maintained in RPMI 1640 supplemented with 10–15% fetal bovine serum (FBS) and 0.1% gentamicin sulfate (GeminiBioproducts, Calabasas, CA). Endometrial cell lines were maintained and propagated in MEM (Ishikawa), McCoy's 5A (Hec1A), and 1:1 D-MEM:F12 (KLE and RL95-2) media supplemented with 10% fetal bovine serum and 0.1% gentamicin sulfate. Spec2 was maintained in a 1:1 mixture of DMEM and Ham's F-12 medium supplemented with 10% fetal bovine serum, L-glutamine, sodium pyruvate, nonessential amino acids, and a 2-fold vitamin solution (Life Technologies Laboratories). Ovcar5 and SKUT2 cells were maintained in D-MEM with 10% and 20% FBS, respectively. Hec1b cells were maintained in MEM supplement supplemented with 10% FBS, glutamine, sodium pyruvate and amino acids. RF-24 cells were maintained in D-MEM supplemented with pyruvate, amino acids, and penicillin/streptomycin.

Cell lines were obtained within one year of the work described, and per institutional policy (MD Anderson policy ACA#1044) cell line authentication was performed at least once per year. In this case, authentication was performed within six

months of the work described. Authentication was performed by the short tandem repeat method using the Promega Power Plex 16HS kit (Promega). Somatic mutations were detected using a Sequenom MALDI TOF MassArray system (Sequenom). Mycoplasma detection was performed using the MycoAlert Kit (Lonza), and all *in vitro* experiments were conducted with 60-80% confluent cultures.

In vivo models

Female athymic nude mice were purchased from Taconic Farms (Hudson, NY) as previously described [59]. The mice were housed and cared for according to guidelines set forth by the United State Public Health Service policy on Human Care and Use of Laboratory Animals and the American Association for Accreditation of Laboratory Animal Care. The University of Texas MD Anderson Cancer Center Institutional Animal Care and Use Committee approved and supervised all studies. All animals were 8–12 weeks old at the time of injection.

Prior to injection of cells for animal experiments, cells were harvested using trypsin-EDTA, FBS-containing media was added, then cells were washed and resuspended in Hanks' balanced salt solution (HBSS; Gibco, Carlsbad, CA) before injection. For the Igrov1 (1×10^6 cells in 200 µl of HBSS), SKOV3ip1 (1×10^6 cells in 200 µl of HBSS) and HeyA8 (250×10^3 in 200 µl of HBSS) model, cells were injected intraperitoneally For the uterine cancer model, Hec1A cells were injected into the right uterine horn (4×10^6 cells in 100 µl of HBSS). For the intra-uterine injections, mice were anaesthetized with ketamine and administered buprenorphine (0.1 mg/kg) subcutaneously. An incision in the midline was made and using blunt dissection the

right uterine horn identified. A 30-gauge needle on a 1-ml tuberculin syringe was used to inject the cell suspension directly into the uterus. After injection, the incision was closed in two layers with 0-0 Vicryl and surgical clips, and the mouse was returned to a cage until fully recovered.

For all experiments, mice were treated by oral gavage daily (25 mg/kg). MSC2363318A was reconstituted in 0.5% Hydroxypropyl Methylcellulose (Hypromellose 2208, Spectrum Chemical), 0.25% Tween 20 in 100 mM Citrate buffer pH3 (Teknova). For the SKOV3ip1, Hec1A, HeyA8, and Igrov1 models, treatments began seven to days after cell injection and continued for approximately four to six weeks. Mice were treated with paclitaxel (4 mg/kg) once weekly via intraperitoneal injection and bevacizumab (6.25 mg/kg) twice weekly via intraperitoneal injection. Once mice in any group became moribund, all mice were sacrificed and necropsied. Tumors were harvested, and weight, number and location of metastatic nodules were recorded. Tumor tissue was preserved and fixed in formalin for paraffin embedding, frozen in optimal cutting temperature media to prepare frozen slides, or snap-frozen for lysate preparation.

Immunoblotting

Lysates were prepared using modified RIPA buffer (50 mM Tris–HCl (pH 7.4), 150 mM NaCl, 1% Triton, 0.5% deoxycholate) plus 25 µg ml^{-1} leupeptin, 10 µg ml^{-1} aprotinin, 2 mM EDTA and 1 mM sodium orthovandate. A BCA Protein Assay Reagent kit (Pierce Biotechnology, Rockford, IL) was used to determine the protein concentrations. Lysates were loaded and then separated on SDS–PAGE. Transfer of

protein was achieved through use of a nitrocellulose membrane by wet electrophoresis (Bio-Rad Laboratories, Hercules, CA) overnight, blocked with 5% BSA for one hour and then incubated at 4°C overnight with primary antibody (p-ribosomal S6 protein 1:1,000, pAKT 1:1000, AKT 1:1000, YAP1 (1:1000); p-p70S6k 1:500, p-70S6k 1:500) (Cell signaling, Danvers, MA)). After washing thrice with tris-buffered saline with Tween 20, membranes were incubated with horseradish peroxidase-conjugated horse anti-Mouse or Rabbit IgG (1:2,000, GE Healthcare, UK) for one hour. Visualization of horseradish peroxidase was performed using an enhanced chemiluminescence detection kit (Pierce Biotechnology). The blots were probed with an antibody specific for β-actin (0.1 µg/mL; Sigma) to confirm equal loading.

Quantitative real-time PCR

Total RNA was isolated using the Qiagen RNeasy kit (Qiagen, CA) and quantified. Complementary DNA was synthesized using 1,000 ng of RNA and a Verso cDNA kit (Thermo Scientific, PA), as per the manufacturer's instructions. A 7500 Fast Real-Time PCR System (Applied Biosystems, CA) with SYBR green-based real-time PCR was used for analysis of mRNA levels for all genes. Specific primers for YAP1 were F-CAAGAAAGCAGGCTCACAGAA, R-GCTGGGTGTTAGGGCTTCG; and 18S F-CGCCGCTAGAGGTGAAATTC, R-TTGGCAAATGCTTTCGCTC were used; 18S was used as a housekeeping gene. PCR was done with reverse-transcribed RNA and 100 ng/µL of sense and antisense primers in a total volume of 20 µL. Each cycle consisted of 15 seconds of denaturation at 95°C and 1 minute of annealing and extension at 60°C (40 cycles).

Cell viability assay

Cell viability assays were performed by testing cell's ability to reduce the tetrazolium salt [3-(4,5-dimethylthiazol-2-yl)-5-(3-carboxymethoxyphenyl)-2-(4-sulfophenyl)-2H-tetrazolium, inner salt] to a formazan. Cells were seeded in a 96-well plate and treated for 96 hours with increasing concentrations of MSC2363318A and paclitaxel and 72 hours with increasing concentrations of bevacizumab. After 96 hours, cells were incubated with 0.15% 3-(4,5-dimethylthiazol-2-yl)-2,5-diphenyltetrazolium bromide (MTT) for 2 hours at 37°C. The supernatant was removed, cells were dissolved in 100-µL DMSO, and the absorbance at 540 nm was recorded.

Immunohistochemistry

Paraffin-embedded tissues were used to detect cell proliferation (with Ki67) and apoptosis (with cleaved caspase-3). Sections were deparaffinized sequentially in xylene and declining grades of ethanol prior to rehydration and transferred to PBS. After antigen retrieval with citrate buffer (pH 6.0), the sections were blocked with 3% hydrogen peroxide in methanol and protein blocker at room temperature. The sections were then incubated with the Ki-67 (1:200; DakoCytomation) and monoclonal mouse antibody against cleaved caspase-3 (1:200; Biocare Medical, Concord, CA) overnight at 4°C. After being washed with PBS, sections were incubated with horseradish peroxidase-conjugated rat anti-mouse immunoglobulin G2a (1:100; Serotec, Harlan Bioproducts for Science, Madison, WI) for Ki67 staining for 1 hour.

CD31 staining was performed on frozen sections. Sections were fixed in cold acetone for 15 min, washed with PBS, blocked with protein blocker (4% fish gel), and

then incubated with rat monoclonal anti-mouse CD31 (1:800, PharMingen, San Diego, CA) overnight at 4°C. After washing the slides with PBS, we added the appropriate horseradish peroxidase–conjugated secondary antibody in blocking solution for one hour at room temperature. Slides were developed with 3, 3"-diaminobenzidine chromogen (Invitrogen, Carlsbad, CA) and counterstained with Gil's No. 3 hematoxylin (Sigma-Aldrich).

For quantification of CD31, Ki67, and cleaved caspase-3 expression, five samples from each group were examined. To quantify microvessel density for each sample, the microvessels within five randomly selected 0.159-mm2 fields at x200 were counted. A single microvessel was defined as a single cell or a discrete cluster of cells stained positive for CD31. To quantify Ki67 expression and cleaved caspase 3, the percentage of positive cells was determined in five random fields at x200 magnification.

In vitro apoptosis assay

For this assay, 150,000 cells were in each well of a six well plate, targeting approximately 50% confluence in serum-containing medium. After daily treatment with IC50 doses of MSC2363318A, cell viability was assessed via flow cytometry using Annexin V and 7-amino-actinomycin-D staining (BD Pharmingen, Franklin Lakes, NJ). Cells were harvested, washed, incubated for 20 minutes with PE-Annexin V and 7-amino-actinomycin-D according to the manufacturer's instructions, and then subjected to flow cytometry.

In vitro proliferation assay

Cells were plated in six well plates with 150,000 cells per well, targeting approximately 50% confluence in serum-containing medium. Cells were treated daily with MSC2363318A using IC50 and IC20 doses. The percentage of proliferating cells (defined as the percentage of cells in S-phase) were determined using the Click-iT EdU flow cytometry kit (Invitrogen). Cells were incubated with 10 mM 5-ethynyl-2-deoxyuridine for 2 hours, lifted, and washed with 1% bovine serum albumin in Dulbecco's PBS. The cells were fixed with 4% paraformaldehyde in Dulbecco's PBS for 15 minutes at room temperature and then maintained for a duration not exceeding 7 days at 4°C in the dark until use. On the day flow cytometric analysis was to be performed, the cells were washed in 1% bovine serum albumin in PBS and permeabilized with 1x saponin-based reagent for 15 minutes at room temperature. Using a solution containing 1x reaction buffer, $CuSO_4$, Alexa-Fluor 488 azide dye, and proprietary reaction buffer additive, the cells were incubated for 30 minutes at room temperature and then subjected to flow cytometric analysis.

Development of resistant RF-24 clone

A bevacizumab-resistant cell line was derived from original parental RF-24 cell line by exposing cells continuously to bevacizumab at (1 mg/mL) for 72 hours. After 72 hours, media was removed and the cells were allowed to recover for seven days. Cells were maintained continuously in the presence of bevacizumab at IC50 concentrations.

Development of YAP1 overexpressing clone

For ectopic expression of YAP1, we obtained a lentiviral plasmid corresponding to a validated full-length wild-type YAP1 from Addgene (PLX304-YAP1-V5, ID: 42555). We transduced Ovca432, Igrov1, and Hec1b cells with virus particles (PLX304-YAP1 and PLX304 empty plasmid control) and then selection using neomycin/G418 (InvivoGen; 600mg/ml) was carried out to establish stable cell variants.

RF-24 tube formation assay

Sensitive and resistant RF-24 cells were seeded at a density of 100,000 per well in a six well plate and allowed to attach overnight. The culture medium was then aspirated and replaced with fresh culture medium containing 0.5 mg/mL and cell lines specific IC50 doses of MSC2363318A. A 96-well plate was coated with 50 µL of Matrigel, which was allowed to solidify at 37°C for ten minutes. Next, 20,000 cells per well were seeded on the Matrigel. The cells were incubated at 37°C for six hours. To assess tube formation, we counted and photographed complete tubes from randomly chosen fields using an Olympus inverted microscope connected to a digital camera.

Statistical Analysis

Continuous variables were compared with the two-sample t test (between two groups) or with analysis of variance (ANOVA; for all groups) if normally distributed (as determined by the Kolmogrov-Smirnov test), and the Mann-Whitney test was used if distributions were nonparametric. A *p*-value of less than 0.05 from a two-tailed

statistical test was considered statistically significant. All statistical tests were two-sided.

Reverse Phase Protein Arrays (RPPA)

Igrov1, Ovcar5, Hec1B, Ishikawa ,RL95-2 KLE, RF-24 cells sensitive to bevacizumab, and RF-24 cells resistant to bevacizumab were treated with 1 µM MSC2363318A for 24 hours and subjected to RPPA as previously described [60,61,62]. Cellular proteins were denatured by 1% SDS (with beta-mercaptoethanol) and diluted in five 2-fold serial dilutions in dilution buffer (lysis buffer containing 1% SDS). The serial diluted lysates were then arrayed on nitrocellulose-coated slides (Grace Biolab) by Aushon 2470 Arrayer (Aushon BioSystems). Total 5808 array spots were arranged on each slide, which included the spots corresponding to positive and negative controls prepared from mixed cell lysates or dilution buffer, respectively.

Each slide was probed with a validated primary antibody plus a biotin-conjugated secondary antibody. Only antibodies with a Pearson correlation coefficient between RPPA and western blotting of greater than 0.7 were used in reverse phase protein array study. Antibodies with a single or dominant band on western blotting were further assessed by direct comparison to RPPA using cell lines with differential protein expression or modulated with ligands/inhibitors or siRNA for phospho- or structural proteins, respectively.

The signal obtained was amplified using a Dako Cytomation–catalyzed system (Dako) and visualized by DAB colorimetric reaction. The slides were scanned,

analyzed, and quantified using a customerized-software Microvigene (VigeneTech Inc.) to generate spot intensity.

Each dilution curve was fitted with a logistic model ("Supercurve Fitting" developed by the Department of Bioinformatics and Computational Biology in MD Anderson Cancer Center, "http://bioinformatics.mdanderson.org/OOMPA"). This fits a single curve using all the samples (i.e., dilution series) on a slide with the signal intensity as the response variable and the dilution steps are independent variable. The fitted curve is plotted with the signal intensities – both observed and fitted - on the y-axis and the log2-concentration of proteins on the x-axis for diagnostic purposes. The protein concentrations of each set of slides were then normalized by median polish, which was corrected across samples by the linear expression values using the median expression levels of all antibody experiments to calculate a loading correction factor for each sample.

Results

PI3K/AKT pathway alterations in ovarian and uterine cancer

To determine the prevalence of PI3K/AKT pathway alterations in ovarian and uterine cancer, TCGA was queried. An oncoprint was developed for high grade serous ovarian cancers to incorporate the genes, *AKT1*, *AKT2*, *AKT3*, *PTEN*, *RPS6KB2*, and *PIK3CA* (Figure 3). The majority of alterations included amplifications of *AKT1*, *AKT2*, *AKT3*, and *PIK3CA*.

Figure 3. PI3K/AKT pathway has genes altered in 47% (n=272) of high grade serous ovarian cancer cases from The Cancer Genome Atlas.
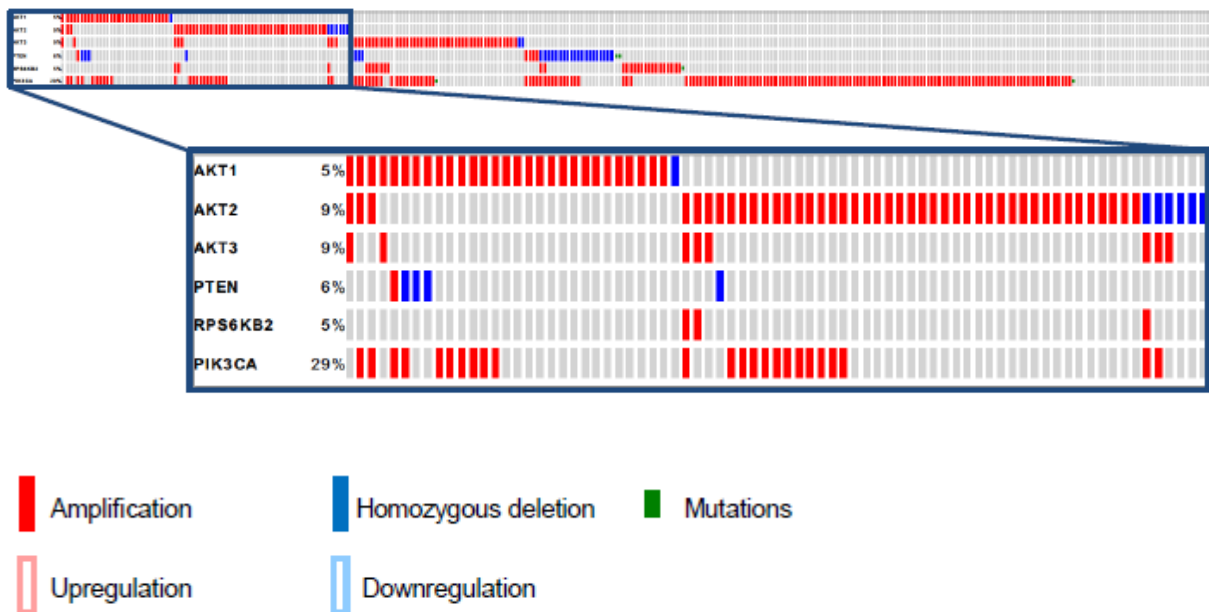
A similar analysis was performed from TCGA for uterine cancer, and an oncoprint was developed with the same genes: *AKT1*; *AKT2*; *AKT3*; *PTEN*; *RPS6KB2*;

and *PIK3CA* (Figure 4). Mutations in *PTEN* and *PIK3CA* were the dominant mutations identified.

Figure 4. PI3K/AKT pathway has genes altered in 90% (n=216) of uterine cases from The Cancer Genome Atlas.

Therapeutic efficacy of MSC2363318A in orthotopic models ovarian and uterine cancer

First, we carried out a dose-finding experiment with MSC2363318A in an ovarian model (Igrov1), whereby mice were treated with varying concentrations of drug after tumors were established. Downstream markers were evaluated after 12, 24, and 48 hours of the last dose administration (Figure 5). A reduction in expression of downstream p-ribosomal S6 protein and resultant increase in pAKT[473] (from feedback

loops) was observed at doses of 20 and 40 mg/kg after 24 hours. Abrogation of this downstream inhibition was seen 48 hours after the last dose was administered.

Figure 5. Dose finding experiments with MSC2363318A in an ovarian orthotopic model. Western blot analysis of downstream markers from tumors of mice inoculated with Igrov1 cells and treated with vehicle, 10 mg/kg MSC2363318A, 20 mg/kg, and 40 mg/kg after 12, 24, and 48 hours after last treatment.
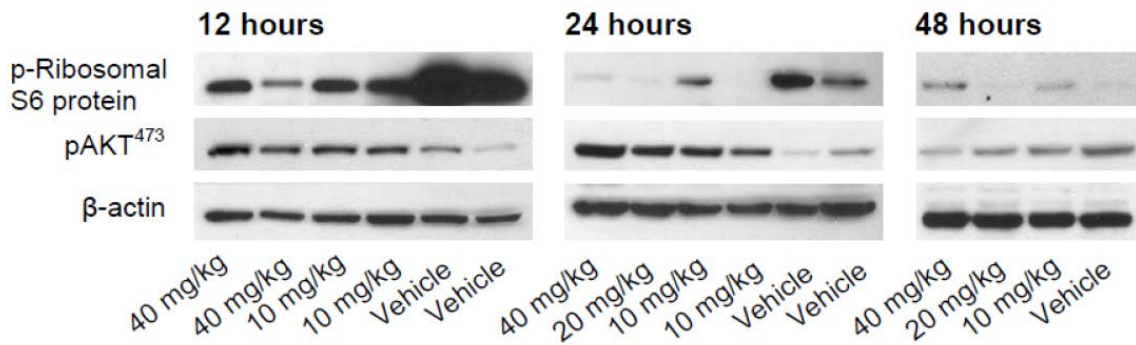
Therefore, daily administration of 25 mg/kg was chosen given the return of downstream markers after 24 hours and the maximum tolerated dose was between 20 and 25 mg/kg alone and in combination with paclitaxel (Figure 6).

Figure 6. Maximum tolerated dose experiment with MSC2363318A monotherapy and in combination with paclitaxel on non-tumor bearing mice. Body weight percentage differences from maximum tolerated dose experiment of non-tumor bearing mice after daily treatment for 14 days with MSC2363318A 20, 25, and 30 mg/kg and 20 and 25 mg/kg combined with paclitaxel (4 mg/kg).
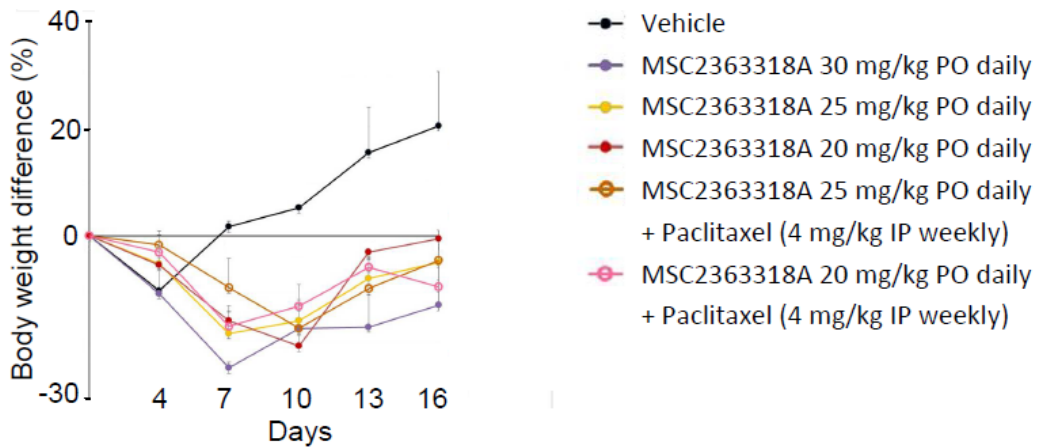
Next, we carried out a series of experiments to characterize the therapeutic efficacy of MSC2363318A on tumor growth alone and in combination with paclitaxel, a commonly used frontline adjuvant therapy in gynecologic malignancies. In the SKOV3ip1 model, treatment with MSC2363318A monotherapy resulted in a 92.8% reduction in tumor weight compared to control (p<0.01) and treatment in the combination group with MSC2363318A paclitaxel resulted 94% reduction in tumor weight (p<0.05) (Figure 7A). Less distant metastases were observed at necropsy in monotherapy and combination therapy groups (Figure 7B-C) and reductions in tumor nodules were observed in all treatment groups (Figure 7D). There was 16-17% decrease in mouse body weight, which was not associated with any noticeable

changes in mobility or feeding habits (Figure 7E). A reduction in downstream p-ribosomal S6 protein was seen in both groups treated with MSC2363318A (Figure 6F).

Figure 7. Effects of MSC2363318A on ovarian tumor growth. Mice were inoculated with (A-C) SKOV3ip1 cells intraperitoneally and received vehicle (control), MSC2363318A (25 mg/kg oral daily), paclitaxel (4 mg/kg intraperitoneally weekly), or a combination of MSC2363318A and paclitaxel. Tumor growth and metastatic locations are shown. (D) Mouse weights, (E) number of metastatic nodules, and (F) western blot analysis of downstream markers from tumors of mice inoculated with SKOV3ip1. Error bars represent the standard error of the mean (SEM). *, P < 0,05; **, P < 0.01; and ***, P < 0.001.
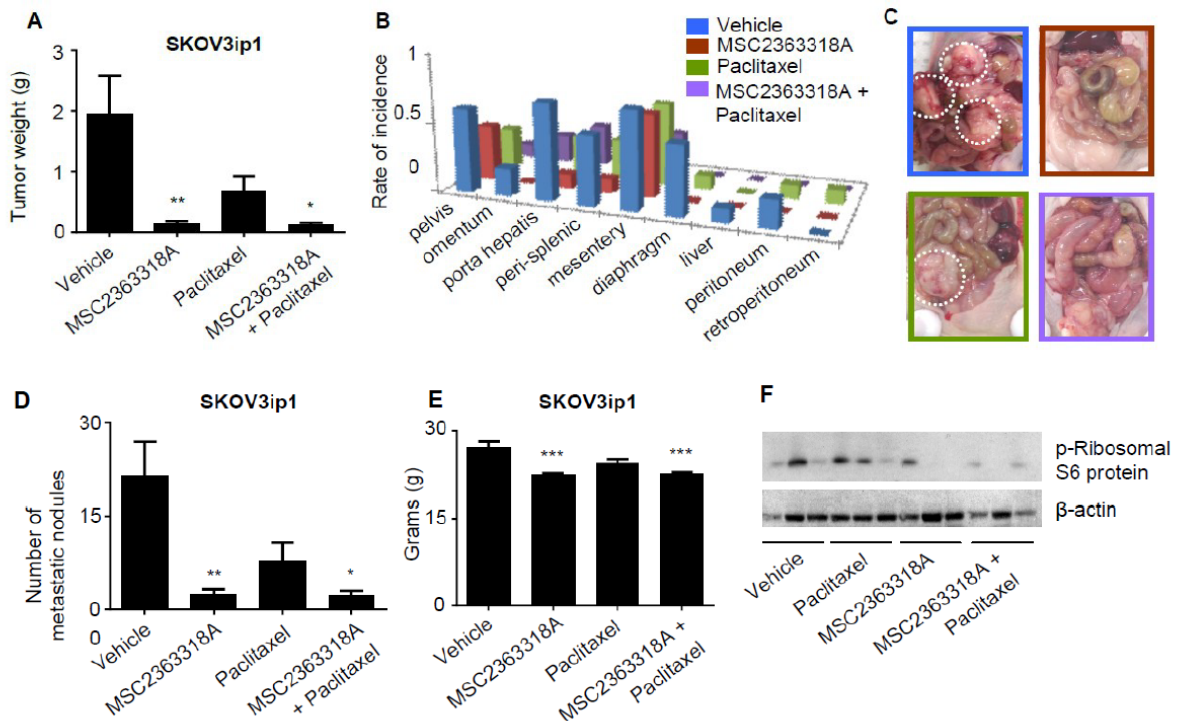
An additional ovarian orthotopic model with Igrov1 was performed (Figure 8A-C) with similar results in tumor growth and metastatic spread. Mice treated with MSC2363318A had decreased weight, and combination MSC2363318A and paclitaxel treated mice had the fewest metastatic nodules (p<0.05) (Figure 8D-E).

Figure 8. Effects of MSC2363318A on ovarian tumor growth in a second orthotopic model. Mice inoculated with (A-C) Igrov1 cells received vehicle (control), MSC2363318A (25 mg/kg oral daily), paclitaxel (4 mg/kg intraperitoneally weekly), or a combination of MSC2363318A and paclitaxel beginning ten days after inoculation. The sites of metastases were recorded and representative pictures are shown. (D) Mouse weights and (E) the number of metastatic nodules were recorded at necropsy. Error bars represent the standard error of the mean (SEM). *, P < 0,05; **, P < 0.01; and ***, P < 0.001.
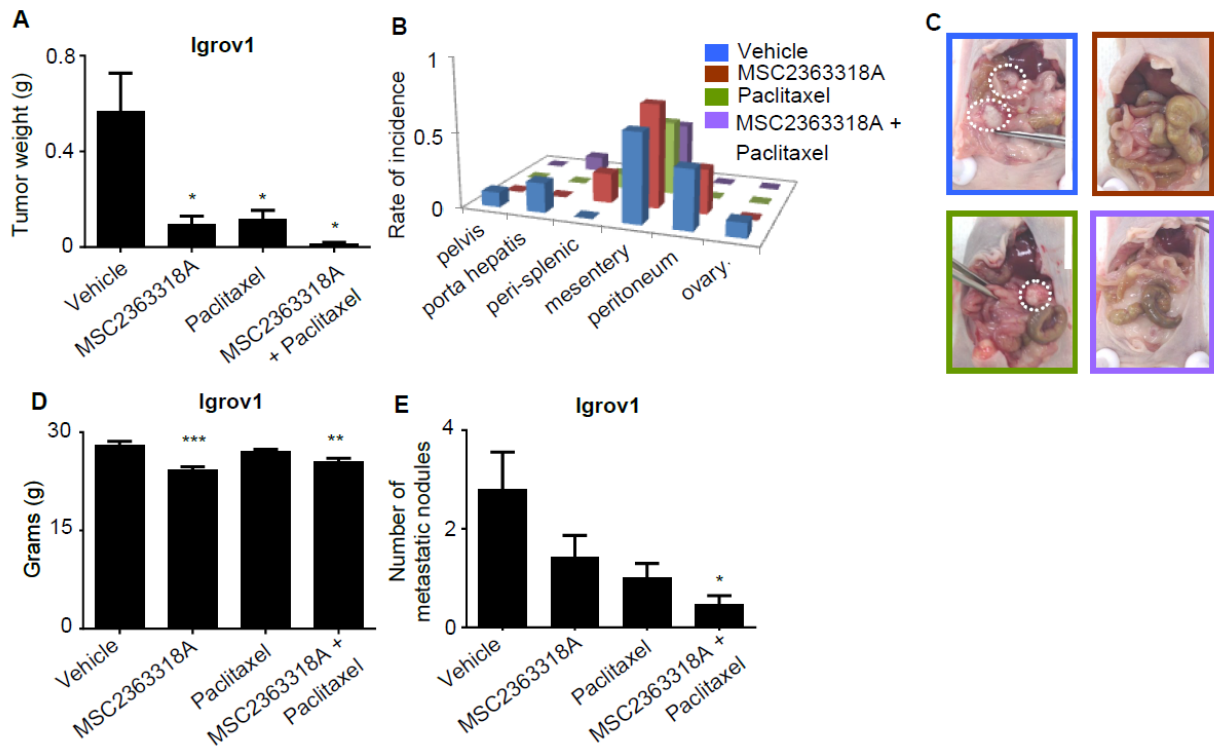
Given the high prevalence of PI3K/AKT pathway activation, we also examined the biological effects of MSC2363318A in a uterine cancer model. Specifically, ten days following inoculation of Hec1a cells into the uterine horn, treatment with MSC2363318A and paclitaxel was initiated. Tumor weight was reduced in all treatment groups, but most significantly in the combination MSC2363318A and paclitaxel treatment group (85.3% reduction, p<0.0001) (Figure 9A). Local spread to the mesentery and within the pelvis and distant liver metastases were observed in all groups (Figure 9B-C).The most significant reduction in distant metastatic sites occurred in combination treatment groups (p=0.0003) (Figure 9D) There was a reduction in mouse weights in the groups treated with monotherapy or combination MSC2363318A and paclitaxel (Figure 9E). A reduction in downstream p-ribosomal S6 protein was seen in both groups treated with MSC2363318A (Figure 9F).

Figure 9. Effects of MSC2363318A on uterine tumor growth. Mice were inoculated with (A-C) Hec1a cells via intrauterine horn injection and received vehicle (control), MSC2363318A (25 mg/kg oral daily), paclitaxel (4 mg/kg intraperitoneally weekly), or a combination of MSC2363318A and paclitaxel. Tumor growth and metastatic locations are shown. (D) Number of metastatic nodules, (E) mouse weights, and (F) western blot analysis of downstream markers from tumors of mice inoculated with SKOV3ip1. Error bars represent the SEM. *, $P < 0.05$; **, $P < 0.01$; ***, $P < 0.001$; and ****, $P < 0.0001$.
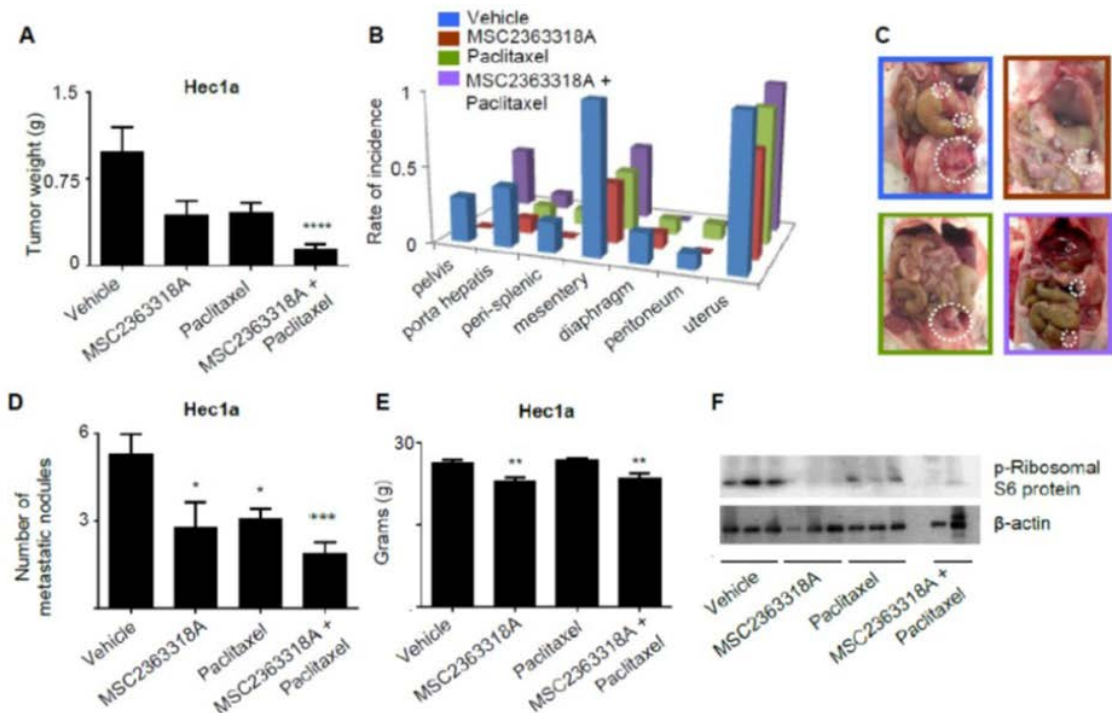
Biological effects of MSC2363318A on proliferation, and apoptosis

Given the robust therapeutic effects of MSC2363318A *in vivo*, we evaluated potential biological effects in tumors collected at necropsy. In the SKOV3ip1 model, treatment with combination MSC2363318A and paclitaxel resulted in the furthest reduction of cellular proliferation as determined by Ki67 (83% reduction, $p < 0.0001$) (Figure 10A). Treatment with MSC2363318A alone or in combination with paclitaxel increased cleaved caspase-3 by more than 62% ($p < 0.0001$) (Figure 10B).

Figure 10. Effect of MSC2363318A on proliferation and apoptosis on ovarian tumors. SKOV3ip1 tumors were collected at the conclusion of *in vivo* therapeutic experiments and immunohistochemical stains were performed to evaluated the effects of MSC23633318A, paclitaxel, or combination therapy on cancer cell (A) proliferation (Ki67) and (B) apoptosis (cleaved caspase-3 [CC3]) staining. Representative sections (final magnification, ×20) are shown for the four treatment groups. The mean Ki67-positive cells and mean cleaved caspase-3 cells are shown in the adjoining graphs. Five fields per slide and at least five slides per treatment group were examined and compared using the Student *t*-test. Error bars represent the SEM. *, $P < 0,05$; **, $P < 0.01$; ***, $P < 0.001$, ****, $P < 0.0001$.
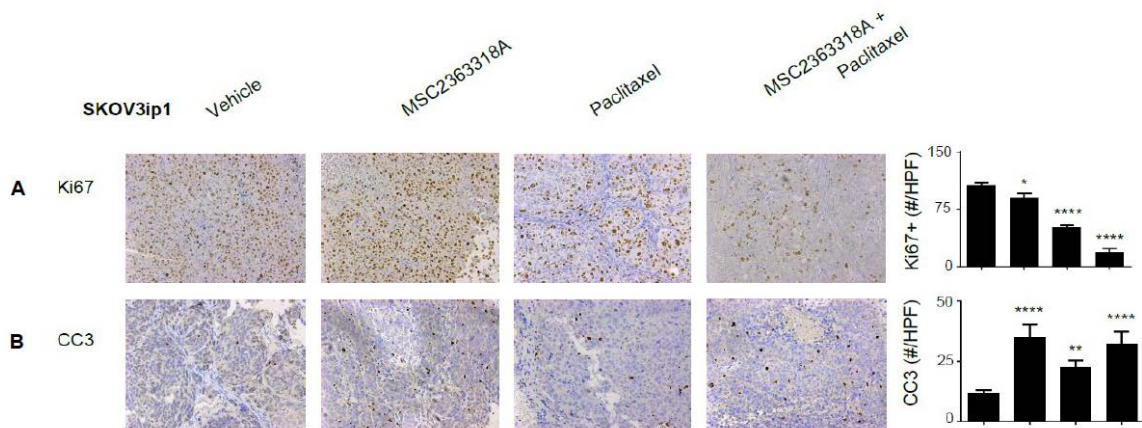
Statistically significant reductions in CD31 ($p<0.05$) and Ki67 ($p<0.0001$) with increases in cleaved caspase-3 ($p<0.001$) occurred in the combination MSC2363318A and paclitaxel treated mice inoculated with Igrov1 cells (Figure 11).

Figure 11. Effect of MSC2363318A on apoptosis, proliferation, and angiogenesis on ovarian tumors. lgrov1 tumors were collected at the conclusion of *in vivo* therapeutic experiments and immunohistochemical stains were performed to evaluated the effects of MSC23633318A, paclitaxel, or combination therapy on cancer cell (A) cancer cell angiogenesis (CD31), (B) proliferation (Ki67), and (C) apoptosis (cleaved caspase-3 [CC3]) staining. Representative sections (final magnification, ×20) are shown for the four treatment groups. The mean Ki67-positive cells, mean cleaved caspase-3 cells, and average number of CD31-positive vessels per field are shown in the adjoining graphs. Five fields per slide and at least five slides per treatment group were examined and compared using the Student *t*-test. Error bars represent the SEM. *, P < 0,05; ***, P < 0.001, ****, P < 0.0001.
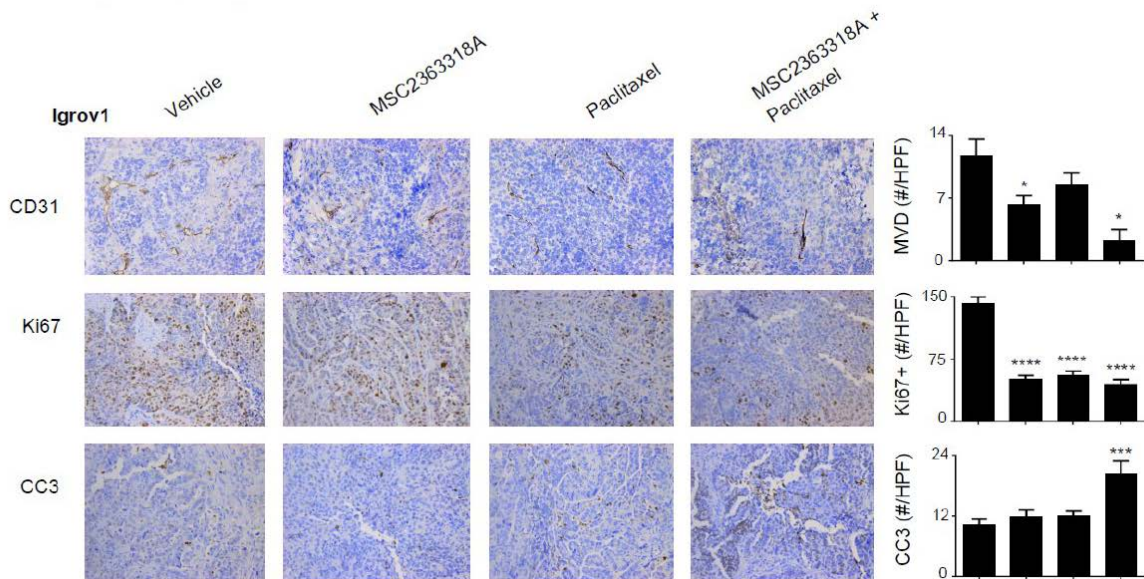
In the Hec1a model, all treatment groups had a statistically significant reduction in Ki67, but this effect was most pronounced in the combination MSC2363318A and paclitaxel group (52.8%, p<0.0001) (Figure 12A). Treatment with MSC2363318A alone

or in combination with paclitaxel led to a 33-45% increase in cleaved caspase-3 (p<0.01) (Figure 12B).

Figure 12. **Effect of MSC2363318A** *on* **proliferation and apoptosis on uterine tumors.** Hec1a tumors were collected at the conclusion of *in vivo* therapeutic experiments and immunohistochemical stains were performed to evaluated the effects of MSC23633318A, paclitaxel, or combination therapy on cancer cell (A) proliferation (Ki67) and (B) apoptosis (cleaved caspase-3 [CC3]) staining. Representative sections (final magnification, ×20) are shown for the four treatment groups. The mean Ki67-positive cells and mean cleaved caspase-3 cells are shown in the adjoining graphs. Five fields per slide and at least five slides per treatment group were examined and compared using the Student *t*-test. Error bars represent the SEM. **, P < 0.01; and ****, P < 0.0001.
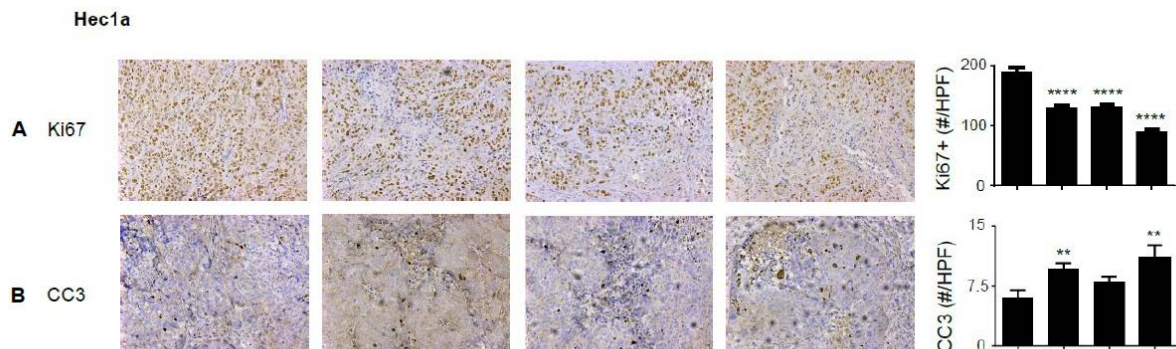
In vitro effect of MSC2363318A in ovarian and uterine cancer cells lines

Cell lines were characterized by mutation status, and we hypothesized that those mutations leading to activation of the PI3K/AKT pathway (such as *PTEN* inactivating mutations and *PIK3CA* mutations) would be the most sensitive to MSC2363318A inhibition (Table 3).

Table 3. Mutation status of ovarian and uterine cancer cell lines [63].

		AKT1	AKT2	AKT3	PIK3CA	RPS6KB2	PTEN
Uterine cancer cell lines	AN3CA	WT	WT	WT	WT	WT	Mut p.R130fs
	Hec1a	WT	WT	WT	Mut p.G1049R	WT	WT
	Hec1b	WT	WT	WT	Mut p.G1049R	WT	WT
	Hec265	WT	WT	WT	WT	WT	Mut p.L318fs
	Ishikawa	WT	Mut p.Y273H	WT	WT	WT	Mut p.E288fs, p.V317fs
	KLE	WT	WT	WT	WT	WT	WT
	RL952	WT	WT	WT	WT	WT	Mut p.M134I, p.R173H
	SKUT2	WT	WT	WT	Mut p.R88Q	WT	Mut p.T321fs, p.V317fs
	Spec2						
Ovarian cancer cell lines	A2780	WT	WT	WT	Mut p.E365K	WT	Mut p.KGR128del
	ES2	WT	WT	WT	WT	WT	WT
	HeyA8	WT	WT	WT	WT	Mut p.T366M	WT
	Igrov1	WT	WT	WT	Mut p.R38C	WT	Mut p.V317fs, p.Y155C
	Ovca432						
	OVCAR3	WT	WT	WT	WT	WT	WT
	OVCAR4	WT	WT	WT	WT	WT	WT
	OVCAR5						WT
	OVCAR8	WT	WT	WT	WT	WT	WT
	SKOV3ip1	WT	WT	WT	Mut p.H1047R	WT	WT

The effect of MSC2363318A on a panel of ten ovarian cancer cell lines was tested and the median inhibitor concentration (IC50) ranged from 0.7 to 12.9 µM (Figure 13). Ovca432 was identified as the most sensitive (IC50 of 0.7 µM) and SKOV3ip1 was the most resistant (IC50 was 12.9 µM).

Figure 13. Effects of MSC2363318A on ovarian cancer cell lines. Cell viability after treatment with MSC2363318A between 0 to 50 µM for 96 hours and mean inhibitory concentration (IC50) after treatment with MSC2363318A in ovarian cancer cell lines. Error bars represent the standard error of the mean (SEM).
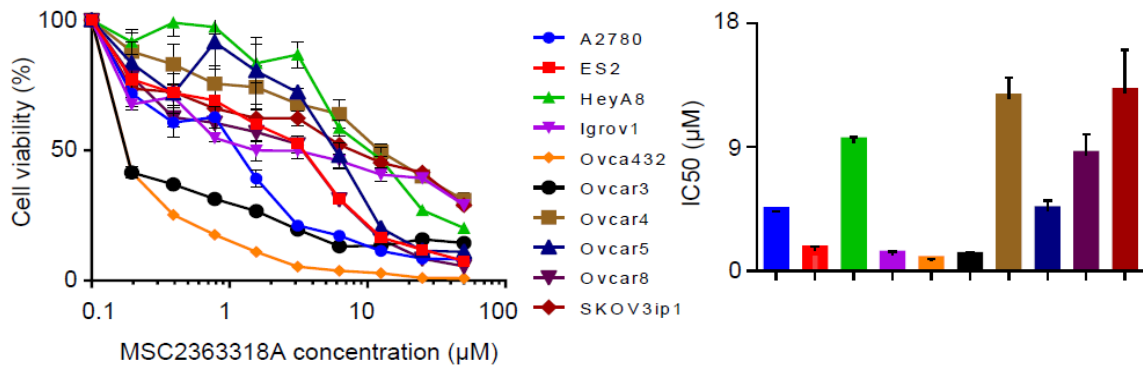
The viability of a panel of nine uterine cancer cell lines were evaluated after treatment with MSC2363318A and the IC50 ranged from 0.0004 to 33.8 µM (Figure 14). AN3CA and KLE were identified as the most sensitive and resistant cell lines, respectively.

Figure 14. Effects of MSC2363318A on uterine cancer cell lines. Cell viability after treatment with MSC2363318A between 0 to 50 µM for 96 hours and mean inhibitory concentration (IC50) after treatment with MSC2363318A in uterine cancer cell lines. Error bars represent the SEM.
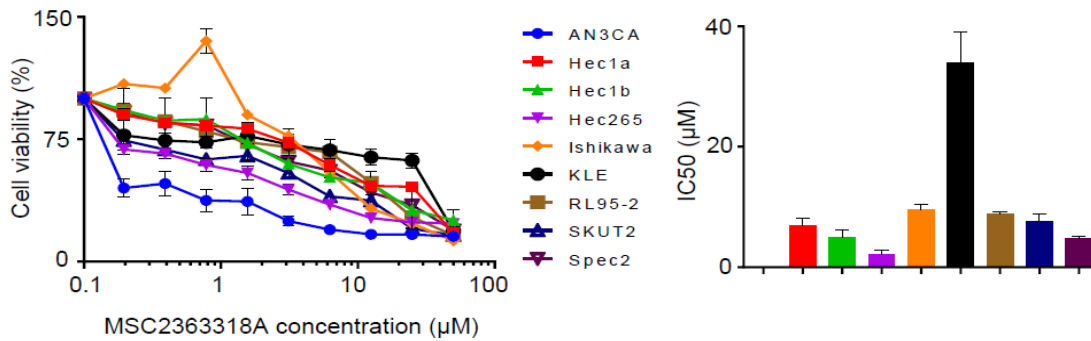
Due to the inhibition of tumor growth and proliferation, we tested these effects *in vitro* using resistant (defined as IC50 $\geq$ 5 µM) ovarian and uterine cancer cell lines, SKOV3ip1 and Ishikawa. We observed significantly decreased proliferation in both cell lines when treated daily at the previously calculated concentrations that inhibited 20% of cell growth (IC20) and IC50 doses (Figure 15).

Figure 15. Effects of MSC2363318A on resistant ovarian and uterine cancer cell line proliferation. Percentage of EdU incorporation in SKOV3ip1 and Ishikawa cells treated daily with control (PBS) and MSC2363318A at cell line specific IC20 and IC50 concentrations measured after 72 hours. Error bars represent the standard error of the mean (SEM). *, P < 0,05; and **, P < 0.01.
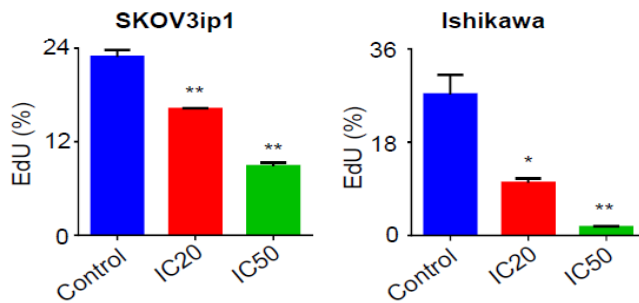
This was also validated in sensitive ovarian and uterine cancer cell lines, Igrov1 and Hec1b, respectively, at both concentrations (Figure 16).

Figure 16. Effects of MSC2363318A on sensitive ovarian and uterine cancer cell line proliferation. Percentage of EdU incorporation in Igrov1 and Hec1b cells treated daily with control (PBS) and MSC2363318A at cell line specific IC20 and IC50 concentrations measured after 72 hours. Error bars represent the SEM. **, P < 0.01.
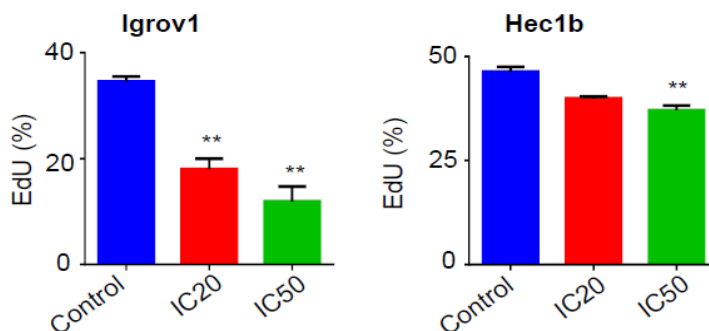
Next, we examined the molecular signaling events involved in the PI3K/AKT pathway after treatment with varying concentrations of MSC2363318A. The expression level of downstream target, p-ribosomal S6 protein, was reduced after treatment in SKOV3ip1 (Figure 17) at concentrations above 100 nM.

Figure 17. Effect of MSC2363318A concentration on downstream markers in the PI3K/AKT pathway. Western blot analysis of downstream and pathway markers after treatment of SKOV3ip1 cells with 0, 0.01, 0.1, 0.5, 1, 5, and 10 µM concentrations of MSC2363318A after 24 hours.
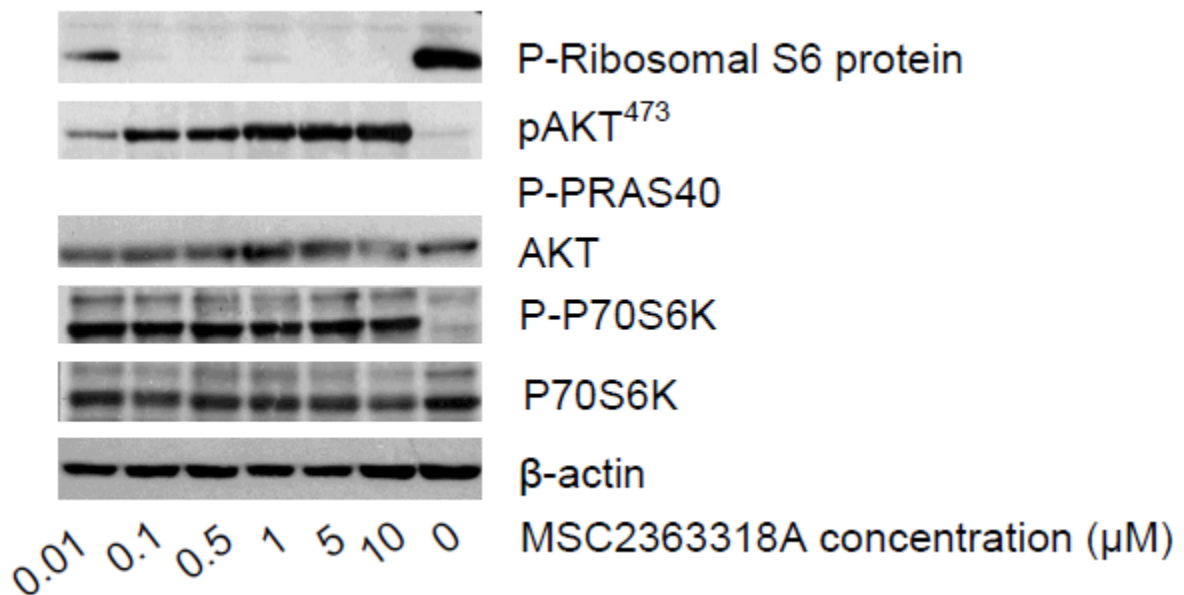
This duration of this effect was between 1 and 24 hours after treatment of SKOV3ip1 cells with 1 µM MSC2363318A (Figure 18).

Figure 18. Effect of time on MSC2363318A on downstream markers in the PI3K/AKT pathway. Western blot analysis of downstream markers after treatment of SKOV3ip1 cells treated with 1 µM MSC2363318A for times specified.
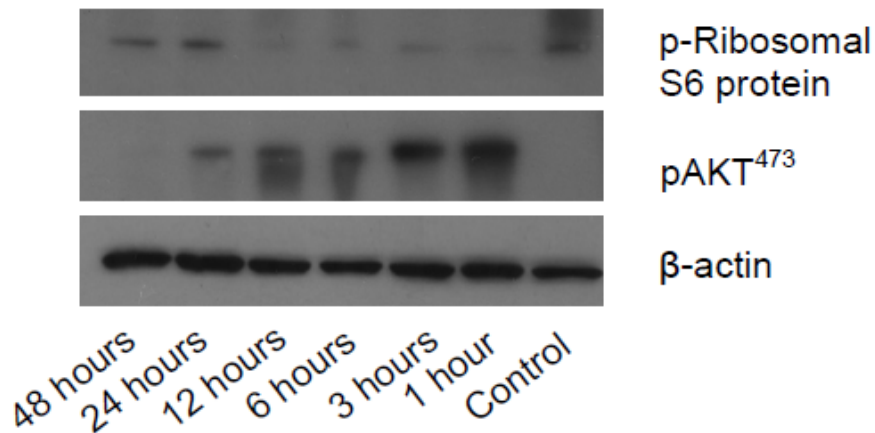
Paclitaxel, a commonly used chemotherapeutic used in the frontline and recurrent setting in ovarian and uterine cancer, was tested in combination with MSC2363318A and contributed to the most profound inhibition of tumor growth and metastases *in vivo*, so the effect of combination treatment was tested *in vitro.* MTT analysis demonstrated a dose-dependent decrease in cell viability after combination therapy with paclitaxel and IC20 and IC50 concentrations of MSC2363118A. The combination index (CI) was obtained after performing an Isobologram analysis, which showed synergistic cytotoxicity in Ishikawa and SKOV3ip1 cells between these two treatments (Figure 19A-B).

Figure 19. *In vitro* **effects of MSC2363318A and paclitaxel in resistant ovarian and uterine cancer cell lines.** (A) SKOV3ip1 and (B) Ishikawa were treated with different concentrations of paclitaxel alone or in combination with the cell line specific IC20 or IC50 for 96 hours followed by MTT analysis to determine percent cell viability. Error bars represent the SEM. The combination index (CI) was calculated after performing isobologram analysis. A CI of < 1.0 indicates synergism, a CI of 1 indicates additive activity and a CI > 1.0 indicates antagonism.
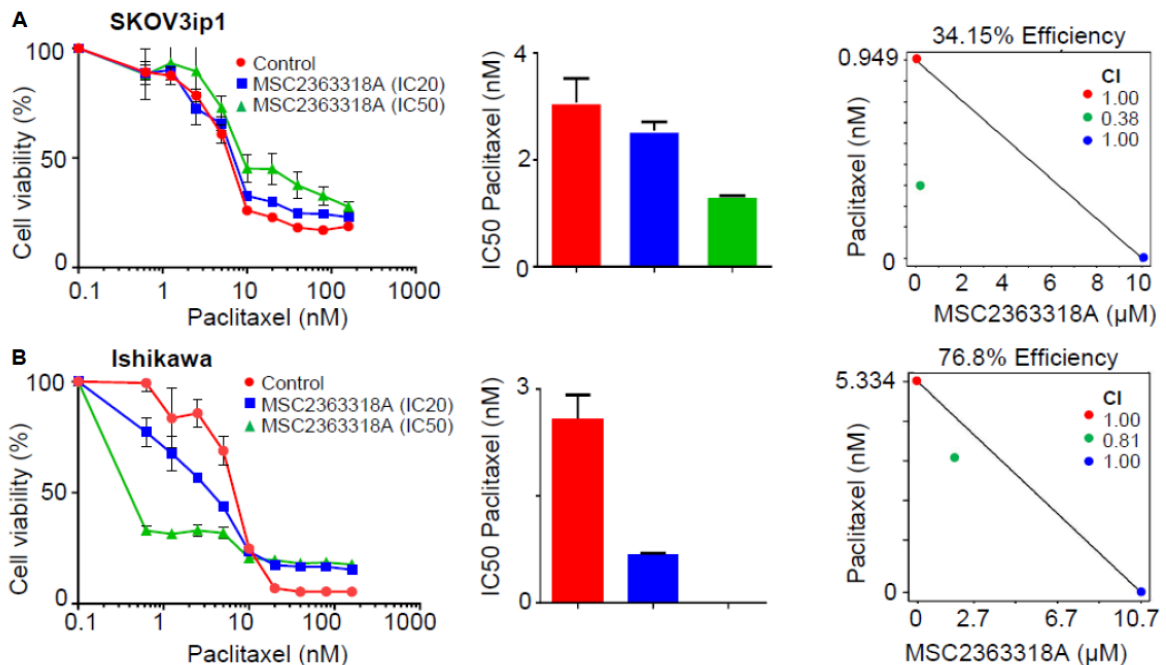
The only other cell line, which showed similar synergy of paclitaxel and MSC2363318A, was in the treatment of uterine cancer cell line, SKUT2 (Figure 20A). Sensitive ovarian and uterine cancer cell lines, Igrov1 and Hec1b, suggested an additive effect when treated concurrently with paclitaxel and MSC2363318A at IC20 and IC50 doses (Figure 20B-C).

Figure 20. *In vitro* effects of MSC2363318A and paclitaxel in sensitive ovarian and uterine cancer cell lines. (A) SKUT2, (B) Igrov1, and (C) Hec1b were treated with different concentrations of paclitaxel alone or in combination with the cell line specific IC20 or IC50 for 96 hours followed by MTT analysis to determine percent cell viability. The combination index (CI) was calculated after performing isobologram analysis for SKUT2. A CI of < 1.0 indicates synergism, a CI of 1 indicates additive activity and a CI > 1.0 indicates antagonism. Error bars represent the SEM.
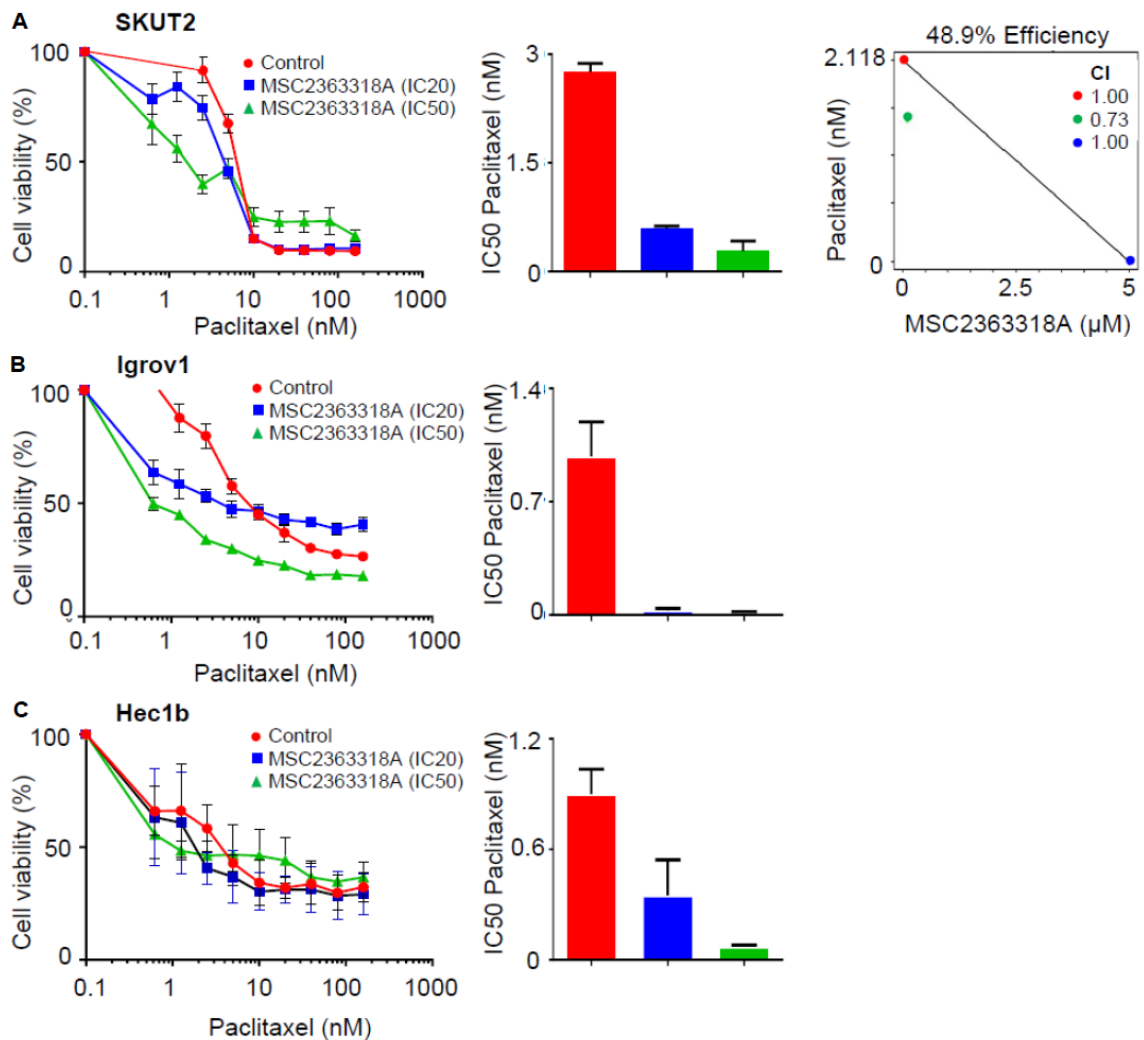
Combination MSC2363318A with paclitaxel also contributed to a statistically significant increase in apoptosis rates in SKOV3ip1 and Ishikawa (Figure 21).

Figure 21. *In vitro* effects of MSC2363318A and paclitaxel in ovarian and uterine cancer cell lines on apoptosis. Apoptosis assay of SKOV3ip1 and Ishikawa cells treated with cell line specific IC50 doses of MSC2363318A, paclitaxel, and combination therapy after 72 hours. Error bars represent the SEM. *, $P < 0,05$; **, $P < 0.01$; and ***, $P < 0.001$.
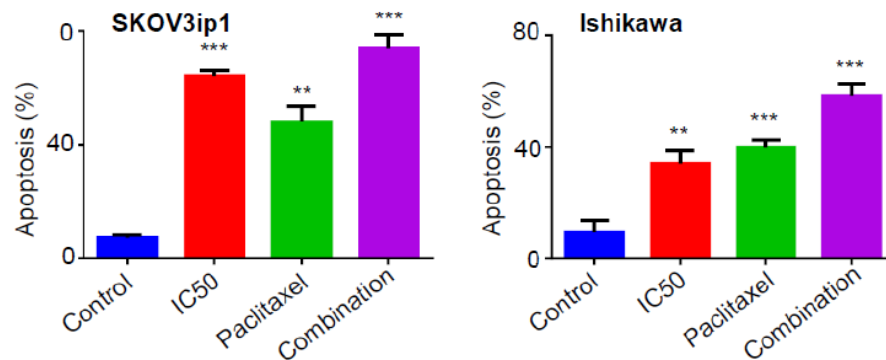
RPPA identifies YAP1 as a predictor of in vitro response to MSC2363318A

To identify potential markers of response to MSC2363318A, we used RPPA to quantify the protein expression of genes that are modulated after treatment in Igrov1 and Ovcar5 ovarian cancer cell lines and Hec1B, Ishikawa, KLE, and RL-952 uterine cancer cell lines (Figure 22).

Figure 22. Differential expression of proteins in the PI3K/AKT/P70S6 signaling pathway after MSC2363318A treatment as detected by reverse-phase protein array. Heatmap of proteins whose expression was different before and after treatment with MSC2363318A (1 µM) for 18 hours.
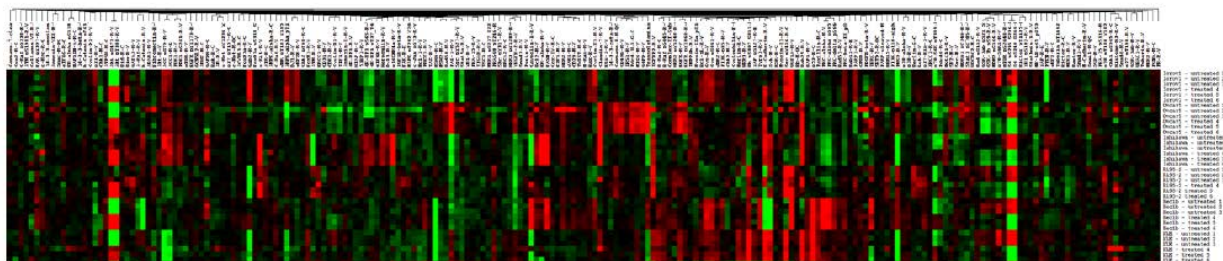
Protein and phosphorylated protein changes were analyzed and uploaded into Ingenuity Pathway Analysis (IPA) to perform a network analysis. We identified the top networks that were activated in the ratio of resistant to sensitive cells lines (Table 4).

Table 4. Top 10 networks in resistant to sensitive ovarian and uterine cancer cell lines.

Diseases or Functions Annotation	p-Value	Predicted Activation State	Activation z-score	# Molecules
metabolism of DNA	2.45E-33	Increased	2.657	44
apoptosis of tumor cell lines	2.61E-71	Increased	2.311	102
degradation of DNA	8.50E-24	Increased	2.240	27
apoptosis of bone cancer cell lines	4.88E-24	Increased	2.238	24
leukocyte migration	4.76E-25	Increased	2.204	52
angiogenesis	2.15E-29	Increased	2.132	52
apoptosis of tumor cells	1.40E-40	Increased	2.060	44
apoptosis of leukemia cell lines	3.91E-37	Increased	2.043	41
cell death of tumor cells	5.34E-40		2.000	48
necrosis of tumor	9.72E-41		2.000	49

Given the robust *in vitro* and *in vivo* effects on angiogenesis, we further investigated the upregulated pro-angiogenic signaling molecules by a network overlaid with the ratio of resistant to sensitive total protein changes (Figure 23).

Figure 23.   Upregulated pro-angiogenic singaling molecules by a network overlaid with the ratio of resistant to sensitive total protein change using Ingenuity Pathway Analysis.
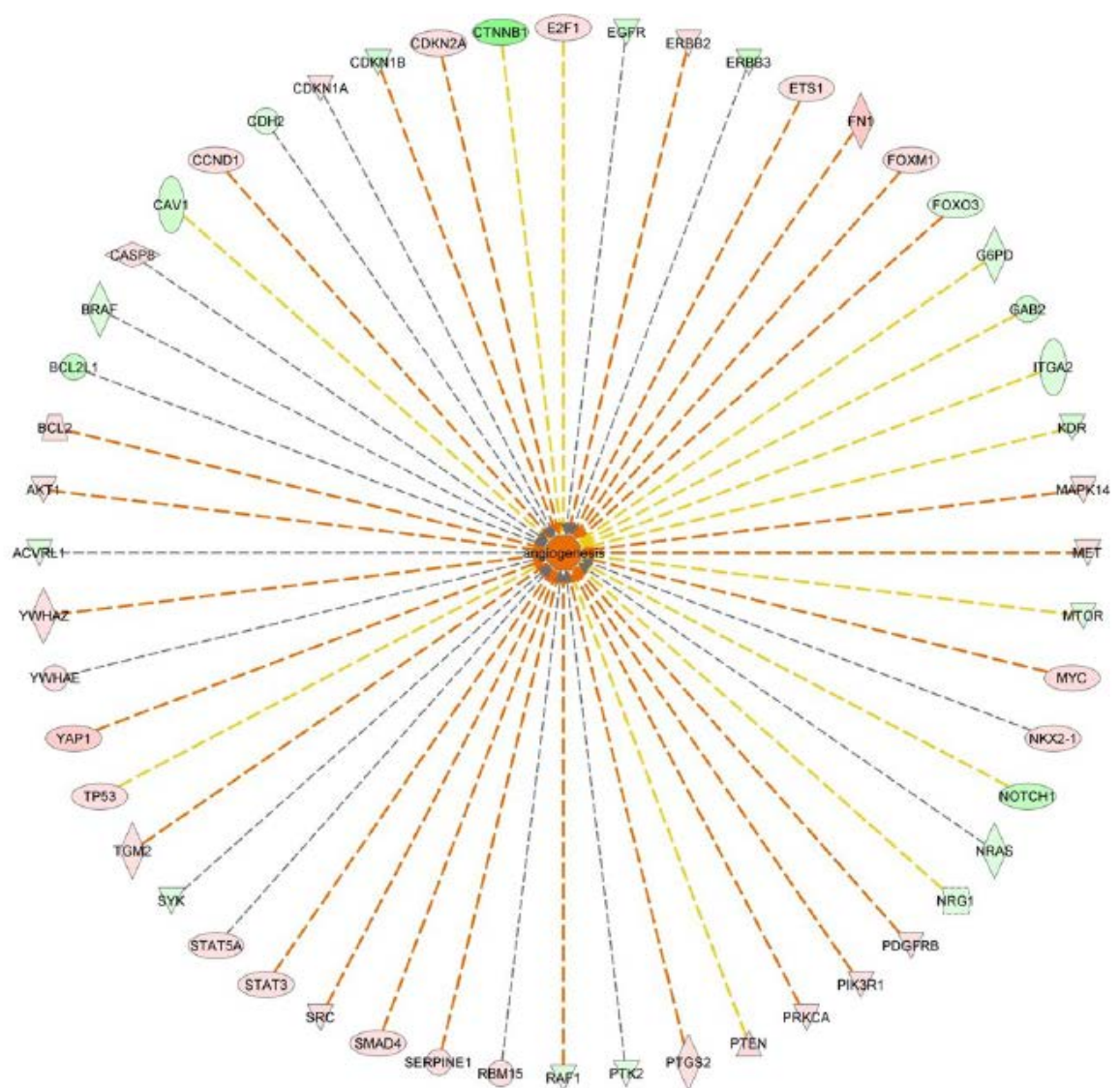
After a further analysis of only resistant cell lines with and without MSC2363318A treatment, we observed an increase in total YAP1 (Figure 24A) whereas in the ratio of treated to untreated sensitive cell lines, there was downregulation of YAP1 (Figure 24B).

Figure 24. Differential expression of angiogenic proteins in the PI3K/AKT/P70S6 signaling pathway after MSC2363318A treatment as detected by reverse-phase protein array. (A) Pro-angiogenic signaling molecules by a network overlaid with the ratio of treated to untreated total protein changes in resistant and (B) sensitive cell lines using Ingenuity Pathway Analysis.
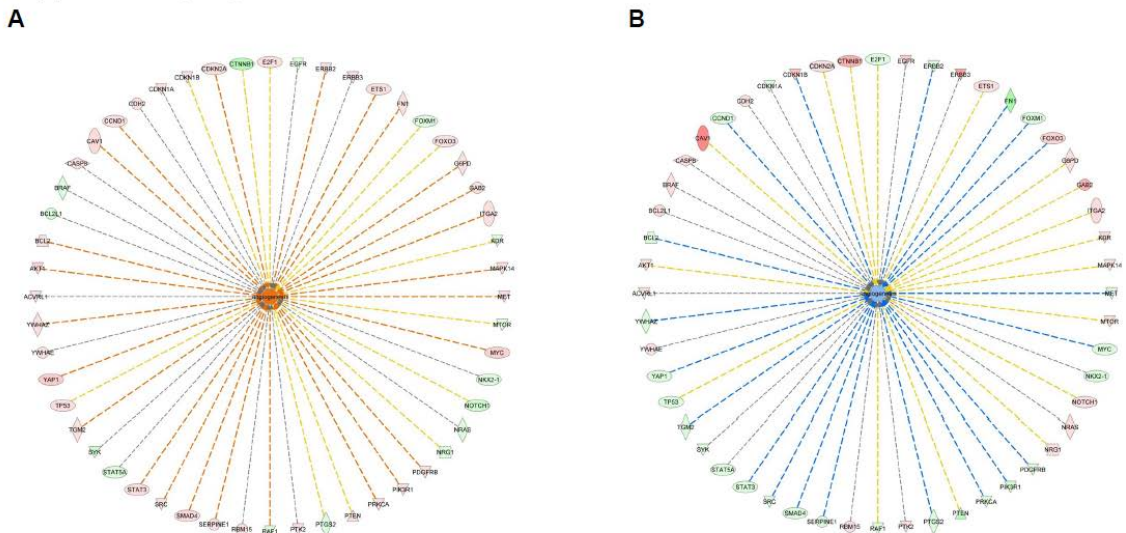
We plotted the logarithmic ratio values for YAP1 and pYAP1 from the cells lines using the RPPA data of the treated over untreated ratio (Figure 25). Total YAP1 was more highly expressed in resistant cell lines.

Figure 25. Logarithmic ratio values for YAP1 and pYAP1 in cancer cell lines. Resistant cell lines were classified by an IC50 ≥ 5 µM. Error bars represent the SEM.
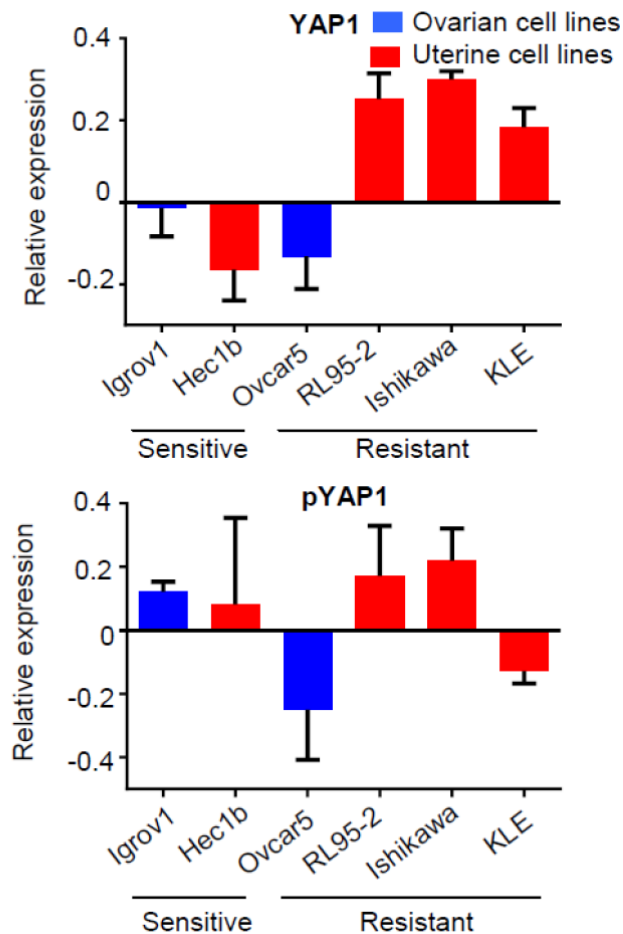
We validated our findings from the RPPA by western blot analysis (Figure 26).

Figure 26. Western blot validation using samples submitted for RPPA.
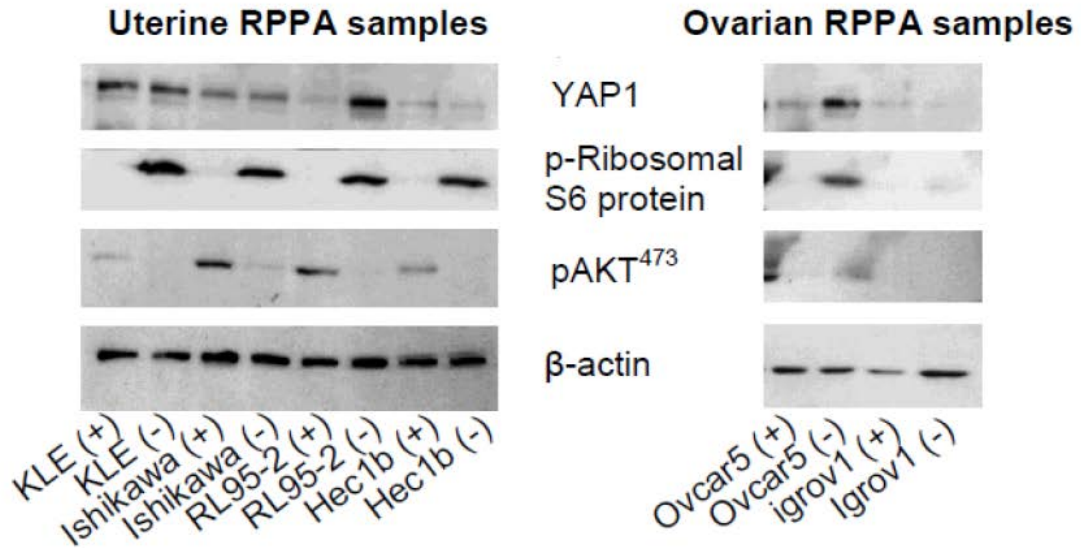
YAP1 expression was evaluated in a panel of ovarian (Figure 27A) and uterine (Figure 27B) cancer cell lines and a Spearman's correlation was performed (R=0.675, p=0.0015), suggesting that more resistant cell lines have higher YAP1 expression and vice versa (Figure 27C). YAP1 expression was also evaluated by western blot (Figure 27D), and there was no association between YAP1 protein expression and IC50 (Figure 27E).

Figure 27. Correlation between YAP1 and MSC2363318A IC50 in ovarian and uterine cancer cell lines. (A) Relative expression of YAP1 in uterine (normalized to post-menopausal endometrial scrapings) and (B) ovarian cancer cell lines (normalized to HIO-180). Quantification was done using the qRT-PCR method. (C) Pearson correlation between YAP1 expression and cell line specific IC50 for MSC2363318A. (D) YAP1 expression in a panel of ovarian and uterine cancer cell lines. (E) Spearman's correlation was performed between YAP1 protein expression and MSC2363318A IC50. Error bars represent the SEM.
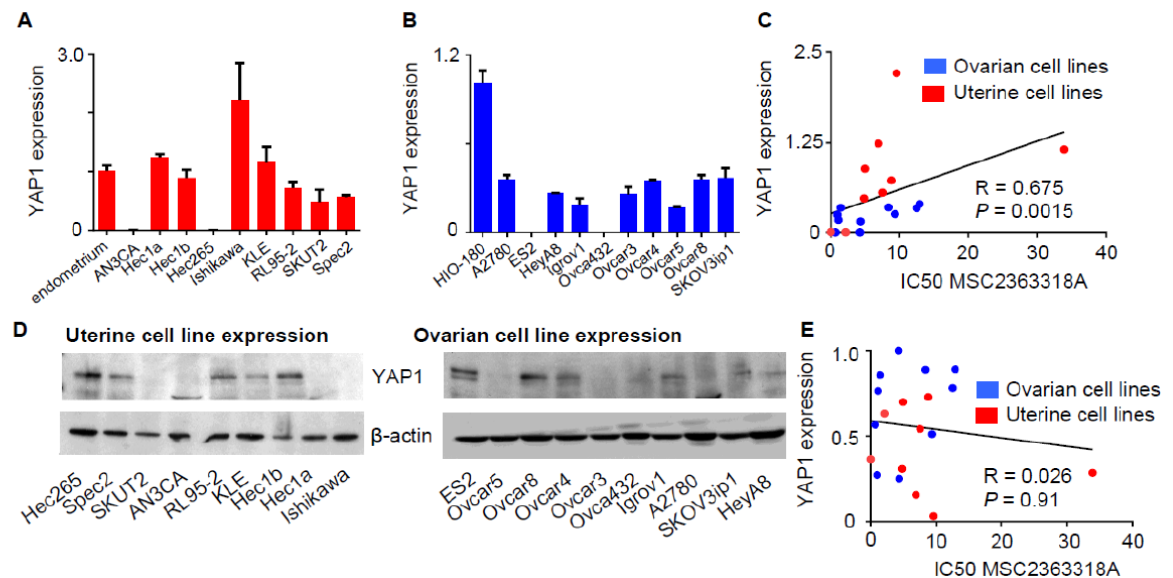
To address the role of YAP1 overexpression and resistance to MSC2363318A, we transfected Ovca432, Igrov1, and Hec1b cells with YAP1 or empty vector and characterized them by western blot (Figure 28A). There were minimal differences in apoptotic rates after treatment with MSC2363318A in the cell lines with empty vector or YAP1 (Figure 28B).

Figure 28. Characterization of YAP1 overexpressing clones and effects on apoptosis after MSC2363318A treatment. (A) Western blot of YAP1 expression in transfected cell lines. (B) Cell viability with Ovca432-plx versus Ovca432-YAP1, Igrov1-plx versus Igrov1-YAP1, and Hec1b-plx versus Hec1b-YAP1 after concentrations of MSC2363318A between 0 and 50 µM were added for 96 hours. Error bars represent the SEM. *, $P < 0{,}05$; **, $P < 0.01$; ***, $P < 0.001$; and ****, $P < 0.0001$.
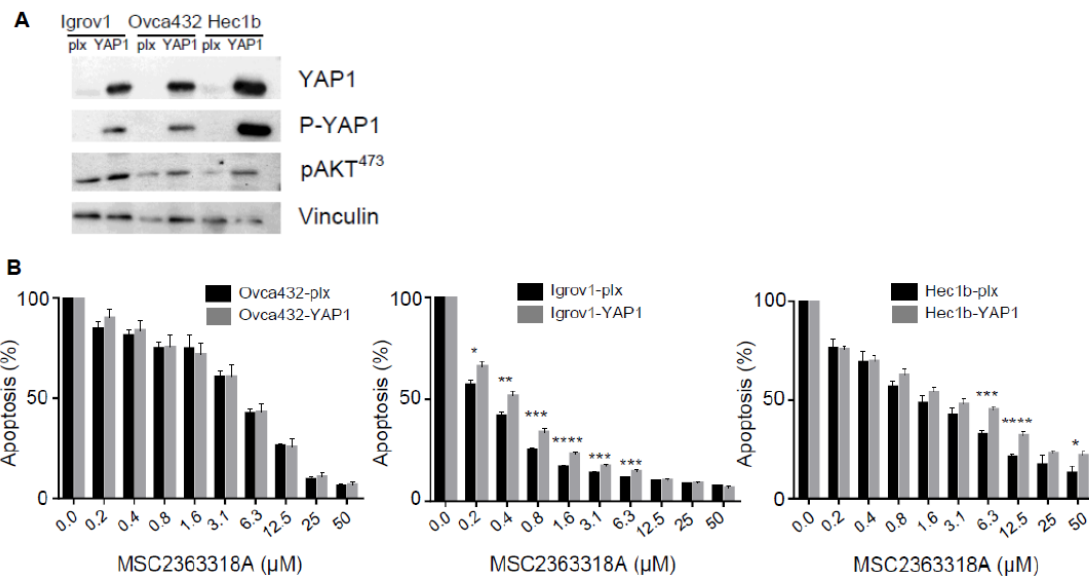
Anti-angiogenic effects of MSC2363318A and bevacizumab

To address whether MSC2363318A affects endothelial cells *in vitro*, we assessed endothelial cell tube formation. Treatment of sensitive RF-24 endothelial cells with MSC2363318A resulted in a 67.2% (p<0.0001) decrease in the number of nodes

formed relative to the control group (Figure 29). Combination MSC23663318A and bevacizumab resulted in an 82.8% reduction (p<0.0001) relative to control.

Figure 29. *In vitro* **effects of MSC2363318A in combination with anti-angiogenic therapy in a sensitive endothelial cell line.** Representative pictures of endothelial vessel formation of sensitive and bevacizumab-resistant RF-24 cells and quantification of the number of number of nodes (points at which where three or more elongated cells meet) formed on the gel matrix after prior treatment with 0.5 µg of bevacizumab, MSC2363318A with the cell line specific IC20, or combination therapy. n = 3 wells per group and mean number of nodes is quantified from five pictures per well. Error bars represent the SEM. ****, P < 0.0001 as determined by the Student t test.

Clinically, patients develop resistance to anti-angiogenic therapies, so we established a bevacizumab resistant RF-24 clone (Figure 30A) to evaluate the effectiveness of MSC2363318A in the resistant setting. Cellular viability was assessed for the sensitive and resistant RF-24 cell lines (Figure 30B) and the sensitive line had a statistically significant lower IC50 (p<0.001). Endothelial cell tube formation was assessed in the resistant RF-24 cell line after treatment with MSC2363318A alone and

in combination with bevacizumab, and there were resultant decreases in the nodes formed in the groups treated with MSC2363318A (Figure 30C).

Figure 30. *In vitro* **effects of MSC2363318A in combination with anti-angiogenic therapy in a resistant endothelial cell line.** (A) Viability of sensitive and bevacizumab-resistant RF-24 cells after treatment with bevacizumab at 0, 0.125, 0.25, 0.5, and 1 µg for 96 hours and (B) MSC2363318A between 0 to 50 µM ± 0.5 mg of bevacizumab for 96 hours and mean inhibitory concentration (IC50). (C) Representative pictures of endothelial vessel formation of bevacizumab-resistant RF-24 cells and quantification of the number of number of nodes (points at which where three or more elongated cells meet) formed on the gel matrix after prior treatment with 0.5 mg of bevacizumab, MSC2363318A with the cell line specific IC20, or combination therapy. $n = 3$ wells per group and mean number of nodes is quantified from five pictures per well. Images were taken at 100× magnification. Error bars represent the SEM. **, $P < 0.01$; and ***, $P < 0.001$ as determined by the Student t test.
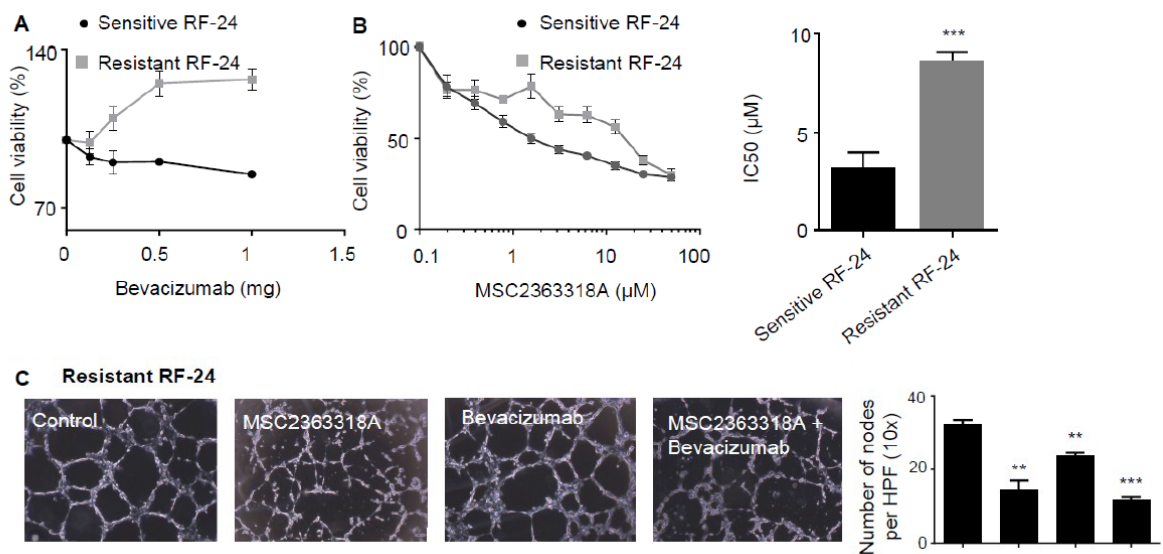
We observed a significant reduction in percentage EdU incorporation in both the sensitive and resistant RF-24 cell lines treated with combination MSC2363318A and bevacizumab suggesting a potentially additive benefit in both the sensitive and resistant setting (Figure 31A). Treatment of resistant and sensitive RF24 cells with 1 µM of MSC2363318A led to a reduction of p-S6 ribosomal protein and increase in pAKT[473] (Figure 31B).

Figure 31. Effect of treatment with MSC2363318A in combination with bevacizumab on proliferation and downstream. (A) Percentage of EdU incorporation in sensitive and bevacizumab-resistant RF-24 cells after treatment without (-) and with (+) bevacizumab and cell line specific IC50 concentrations of MSC2363318A after 72 hours. (B) Western blot of downstream markers after sensitive and resistant RF-24 cells were treated with 1 µM MSC2363318A for 24 hours.
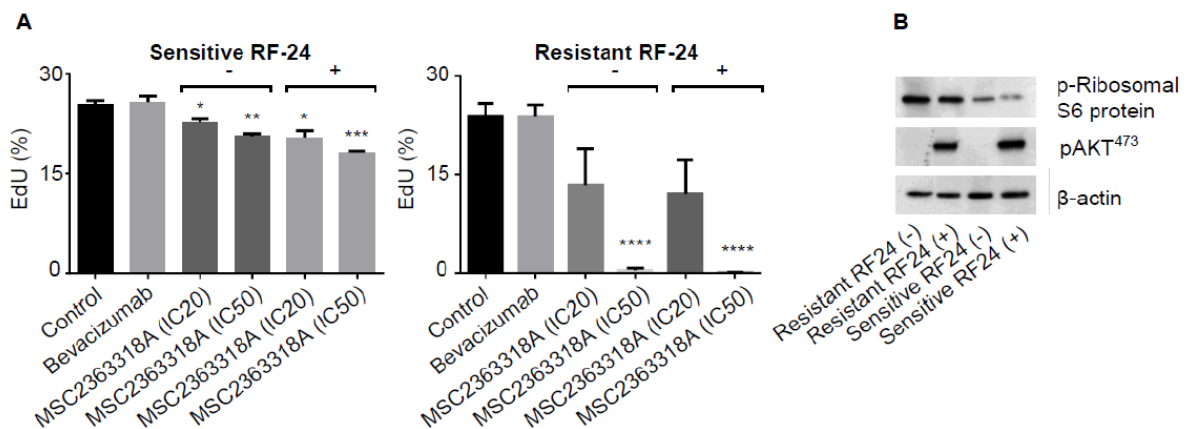
The addition of MSC2363318A and bevacizumab to resistant RF-24 cells led to a 78.5% reduction in the MSC2363318A IC50, which became less than the MSC2363318A IC50 of sensitive RF-24 cells (Figure 32).

Figure 32. Effect on MSC2363318A IC50 in resistant and sensitive RF-24 cells with and without bevacizumab. Viability of sensitive and bevacizumab-resistant RF-24 cells after treatment with MSC2363318A between 0 to 50 µM ± 0.5 mg of bevacizumab for 96 hours and mean inhibitory concentration (IC50). Data represent average of triplicate measurements and error bars represent the SEM. ****, P < 0.0001 as determined by the Student *t* test.
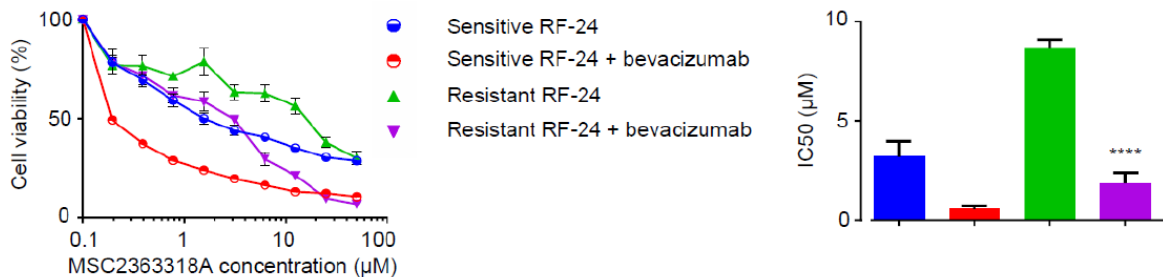
Given the effects of MSC2363318A on angiogenesis *in vitro*, we evaluated the effects on angiogenesis *in vivo* by calculating the microvessel density (MVD) of tumors harvested at the conclusion of the therapy experiments. In the SKOV3ip1 tumor model, treatment with MSC2363318A alone or in combination with paclitaxel decreased MVD by 61.8% (p<0.05) and 63.1% (p<0.01), respectively (Figure 33A). Similar effects of CD31 were observed in the Hec1a orthotopic murine model with significant reductions

in MSC2363318A (36%, p<0.05) and combination MSC2363318A groups (32.4%, p<0.05) (Figure 33B).

Figure 33. *In vivo* effects of MSC2363318A on angiogenesis in combination with paclitaxel. Immunohistochemistry was performed to evaluate the effects of MSC23633318A, paclitaxel, or combination therapy on cancer cell angiogenesis (CD31). Representative sections (final magnification, ×20) are shown for the four treatment groups with the average number of CD31-positive vessels per field in mice inoculated with SKOV3ip1 (A) and Hec1a (B). Error bars represent the SEM. *, P < 0,05; **, P < 0.01.
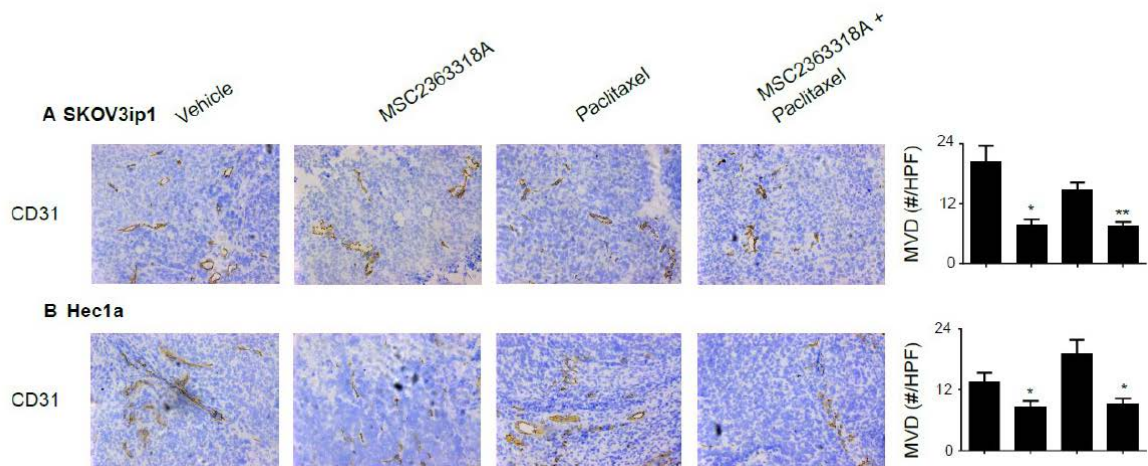
We further investigated the effects of MSC2363318A in combination with an anti-angiogenic therapy, bevacizumab. Substantial reductions in tumor weight were observed in all groups but most profound (96% reduction compared to control, p<0.0001) in the group treated with MSC2363318A and bevacizumab (Figure

34A). Less distant metastases were observed in monotherapy and combination therapy groups (Figure 34B-C). A significant reduction in mouse weight was present in the combination bevacizumab and MSC2363318A group (Figure 34D). Tumor nodules were significantly decreased observed in all treatment groups Figure 34E).

Figure 34. *In vivo* effects of MSC2363318A in combination with anti-angiogenic therapy in an ovarian orthotopic model. Mice inoculated with (A-C) HeyA8 ovarian cancer cells received vehicle (control), MSC2363318A (25 mg/kg oral daily), bevacizumab (6.25 mg/kg intraperitoneally twice weekly), or a combination of MSC2363318A and bevacizumab beginning ten days after inoculation. Tumor size and sites of metastases were recorded and representative pictures are shown. (D-E) Mouse weights and number of metastatic nodules from mice inoculated with HeyA8 received vehicle, MSC2363318A, bevacizumab, or a combination of MSC2363318A and bevacizumab beginning ten days after inoculation. Error bars represent the SEM. *, $P < 0,05$; **, $P < 0.01$; ***, $P < 0.001$; and ****, $P < 0.0001$.
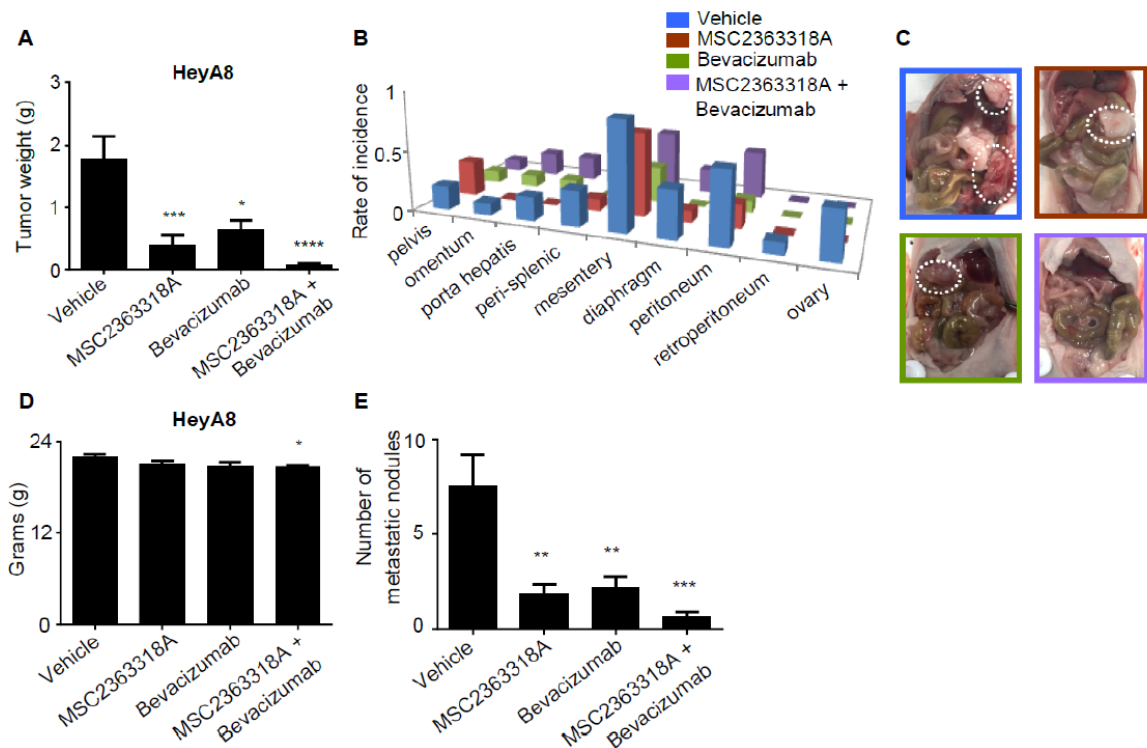
In the HeyA8 tumors, there was a 57.7% (p<0.05) and 59.5% (p <0.01) reduction in MVD in the MSC2363318A monotherapy and combination therapy groups,

respectively (Figure 35). Similar to the other orthotopic models, treatment with MSC2363318A and bevacizumab resulted in decreased cellular proliferation and increased apoptosis (Figure 35).

Figure 35. Effects of MSC2363318A and bevacizumab on angiogenesis, proliferation and apoptosis in an ovarian orthotopic model. Immunohistochemistry was performed to evaluate the effects of MSC23633318A, bevacizumab, or combination therapy on MVD (CD31), proliferation (Ki67), and apoptosis (cleaved caspase-3 [CC3]) staining. Representative sections (final magnification, ×20) are shown for the four treatment groups. Mean Ki67-positive cells mean cleaved caspace-3 cells, and average number of MVD are shown in the adjoining graphs. Five fields per slide and at least five slides per treatment group were examined and compared using the Student t-test. Error bars represent the SEM. *, $P < 0,05$; **, $P < 0.01$; ***, $P < 0.001$; and ****, $P < 0.0001$.
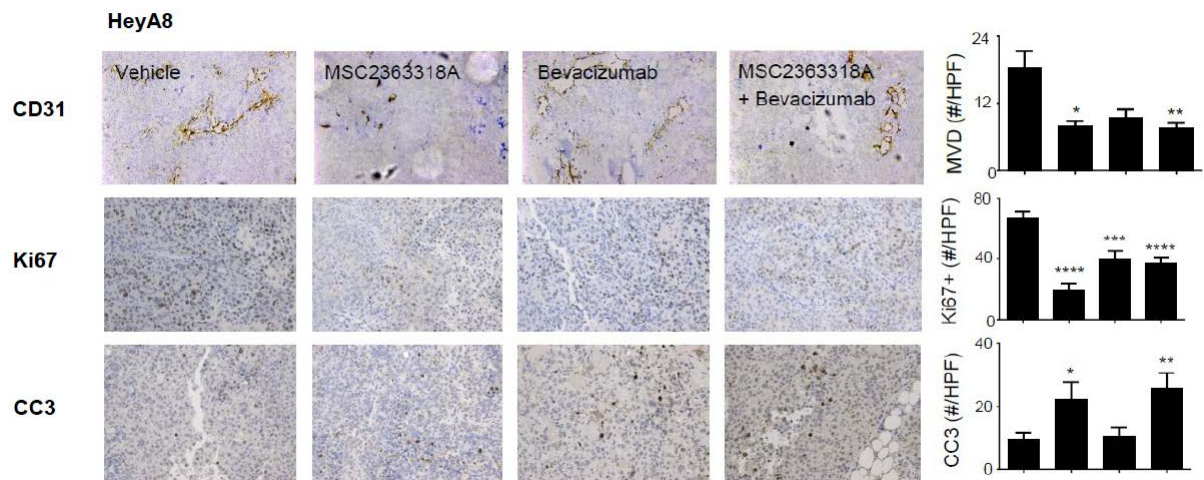
Discussion

The key findings in this manuscript are that dual inhibition of AKT and P70S6K by the novel inhibitor, MSC2363318A, has therapeutic efficacy in multiple preclinical models by enhancing cellular apoptosis, inhibiting proliferation, and reducing the formation of vasculature. Synergy was observed in both cancer types with the combination of MSC2363318A and paclitaxel. Addition of MSC2363318A to anti-angiogenic therapy potentiated the effects of bevacizumab and restored sensitivity in the resistant setting. Finally, we identified YAP1 as a predictor of sensitivity to inhibition with MSC2363318A.

The frequent activation of the PI3K/AKT pathway in malignancies makes it a desirable target for therapeutic intervention. The first drugs developed to target this pathway and approved for treatment included the rapamycin analogs, which included temsirolimus and everolimus. Mechanistically, the drugs allosterically inhibit mTORC1. Other broad classes of inhibitors that have since been developed: (1) ATP competitive dual inhibitors of class I PI3K and mTOR, (2) PI3K inhibitors that inhibit all four class I PI3K isoforms (α, β, δ, and γ); (3) specific PI3K isoform inhibitors; (4) ATP competitive inhibitors of mTOR; and (5) AKT allosteric and catalytic inhibitors [64].

The first PI3K inhibitors, including Wortmannin and LY294002, could bind all class I PI3Ks and lead to pan-inhibition of this pathway. Due to their poor selectivity and pharmacokinetic properties, their therapeutic potential remained limited [27]. Recent pan-class I inhibitors include GDC-0941, BKM120, and PX866. All of these are being tested in ongoing trials for solid and hematologic malignancies including breast, colorectal and squamous cell carcinomas, melanoma, and lymphomas [27]. Second

generation PI3K inhibitors targeted specific PI3K isoforms and are being evaluated in preclinical and clinical studies. GDC-0032 is specific for PI3Kα, which may spare patients from commonly experienced metabolic abnormalities [65,66]. GSK2636771, specific for the PI3Kβ isoform, has been studied in a variety of solid malignancies, especially those that lack PTEN [67]. IPI-145 has been tested in several hematologic malignancies because it preferentially targets PI3Kδ and PI3Kγ, which are the two isoforms that are preferentially expressed on leukocytes [68]. CAL-101, which is PI3Kδ specific, has been tested in acute myelogenous leukemia, chronic lymphocytic lymphoma, Hodgkin's lymphoma, non-Hodgkin's lymphoma, and multiple myeloma [69].

The third generation included dual PI3K/mTOR inhibitors, which target PI3K class I isoforms, mTORC1, and mTORC2, which led to greater inhibition of this entire pathway (19). For example, NVP-BEZ235, has been tested in renal cell and breast cancers. This drug inhibits both ATM and DNA-PKcs and is considered to also be a radiosensitizer. Its lack of bioavailability has prevented further development [70,71].

Three isoforms of AKT possess biologic relevance in cancer pathogenesis and phosphorylation activates multiple downstream signaling cascades including TSC2 protein, TSC1, mTOR, BAD, and caspase-9 (20). AKT inhibitors in preclinical and clinical development include perifosine, a phospholipid derivative of alkylphosphocholine, MK-2206, an allosteric inhibitor of AKT, RX-0201, 20-mer antisense oligodeoxynucleotide directed against AKT, Erucylphosphocholine, PBI-05204, GSK690693, and XL-418 (21). XL-418, which inhibited both AKT and P70S6K,

was tested in a phase I clinical trial in patients with advanced solid tumors. This study was ended due to low drug exposure (NCT00460278).

Successful targeted therapy depends on identifying biomarkers that can be used further during clinical development. This helps to identify which patients are most likely to respond while avoiding untoward toxicities in those patients who will not [72]. Previous data has identified gain of function mutations in *PIK3CA* may cause a tumor to be more sensitive to PI3K inhibition [67]. Up to 91% of uterine cancers may harbor a mutation or alteration in *PTEN*, which contributes to activation of the PI3K/AKT pathway [22]. This may explain why KLE, which is wild type for *PTEN* and *PIK3CA*, may be the most resistant among the uterine cell lines tested. Furthermore, Hec1b has a mutation in *PIK3CA*, but not *PTEN*.

Despite the large number of inhibitors developed to target to this pathway, none of these is able to induce a durable complete remission. This is largely due to resistance that develops and the lack of understanding behind what drives the molecular basis of resistance, whether it is acquired or intrinsic. Proposed mechanisms of resistance include secondary mutations, crosstalk between other pathways that then activate survival mechanisms, and/or amplification of downstream targets within the same targeted pathway [73]. Resistance to PI3K/AKT inhibitors under current development has been linked to the negative feedback loops. Within one of these loops, inhibition of mTORC1 leads to the upregulation of tyrosine kinase receptors (such as platelet derived growth factor receptor [PDGFR] or insulin receptor substrate-1 [IRS-1]). This leads to an increase in phosphorylation of AKT at the serine473 residue. Within a second loop, inhibitor of mTORC1 leads to further PI3K-Ras activation, which

thereby increases the activation of the MAPK pathway [74]. Activation and amplification of MYC may also contribute to inherent resistance of therapeutics that targets this pathway. This parallel pathway may have increased MYC activation through PDK-1 dependent MYC phosphorylation and abrogate the effects of an inhibitor of the PI3K/AKT pathway [75]. This feedback inhibition provides the rationale for further development of MSC2363318A, which inhibits AKT1, AKT3, and P70S6K. Dual inhibition of AKT and further downstream abrogates the negative feedback loop activation that earlier inhibitors of this pathway caused.

One of the most important issues to consider during drug development remains drug toxicities, side effects, and potentially "off-target" effects. The majority of side effects related to therapeutics targeting the PI3K/AKT pathway have been mild to moderate and able to be managed with supportive, expectant management alone [76]. The reported dose limiting side effects from early clinical trials include hyperglycemia, gastrointestinal side effects (including nausea, vomiting, diarrhea, and anorexia), stomatitis, and maculopapular rash [77]. Some of these side effects can be considered "off-target," however most are related to the primary mechanism of action. For example, PI3K inhibitors cause hyperglycemia because this pathway is involved in the insulin signaling pathway. Side effects warrant careful attention and may be useful during dose escalation studies and further clinical decision making [78]. Dual inhibitors of PI3K and mTORC1/2 have been reported to cause a wider variety of off-target effects, such as elevated transaminases and fatigue, but their utility has not been hampered. During our treatment with MSC2363318A, we observed weight loss in the mice receiving treatment, but no behavioral effects or direct side effects were observed.

Our preclinical data indicate that MSC2363318A promotes apoptosis, inhibits proliferation, and restores sensitivity to bevacizumab resistant tumors in both ovarian and uterine cancer. The first phase I trial that is an open-label, non-randomized, dose escalation, trial to explore the safety, tolerability, pharmacokinetic, pharmacodynamics, and clinical activity of MSC2363318A in patients with advanced malignancies has recently opened (NCT01971515). While the niche of this compound remains undetermined, future directions include administration of MSC2363318A as an adjuvant therapy in combination with taxane-based therapy after surgical cytoreduction. Other alternatives include combining MSC2363318A with bevacizumab or other anti-angiogenic therapies in patients whose tumors have developed resistance so that sensitivity to bevacizumab can be restored. Finally, the identification of high YAP1 expression identifies those tumors that are most sensitive to inhibition by MSC2363318A. By identifying the subset of patients whose tumors would be most sensitive to dual AKT/P70S6K inhibition, lower treatment doses could be considered, overtreatment of patients who would not benefit will be avoided, and untoward toxicities in patients who will not respond, would be prevented.

Future directions and translational relevance

The challenge of targeted therapies directed toward the PI3K/AKT pathway is multifaceted. With the advent of so many inhibitors, a rational approach should be developed to determine in which contexts each inhibitor should be used. This would include clinical and prognostic factors as well as the genomic composition of the tumors.

With regard to translating my research findings into clinical trials, rational combinations should be considered and whether a PI3K/AKT inhibitor should be added to standard of care chemotherapy in the adjuvant setting. One way in which this can be evaluated is through "window-of-opportunity" trials. In this trial design, women with newly diagnosed ovarian cancer (as confirmed by pathologic biopsy), would receive a study drug such as MSC2363318A for one to two weeks between the time of biopsy and surgical resection. This allows for physician-scientists to evaluate the targets modulated by the study drug after a given period of exposure time and determine if additional modifications to clinical development should be considered. Additionally, pharmacokinetic assessments can be made on post-resection samples. Alternatively, if the woman received neoadjuvant therapy instead of upfront surgical resection, the biological agent can be added along with traditional chemotherapy for a longer period of time prior to surgery. One of the primary reasons alternative clinical trial designs must be considered is that traditional ways of evaluating response through Response Evaluation Criteria in Solid Tumors (RECIST) criteria, invalid conclusions may be reached about the potential benefit of an investigational agent. Pre-surgical studies such as these may further expedite approval of these agents because they shed light on the biologic effect of the drug early in the development, rather than waiting for the results of Phase II and III studies. Furthermore, they contribute to the validation of markers that will help clinicians identify which patients will best benefit from this type of therapy. Other possibilities include use of inhibitors as a maintenance therapy after complete surgical resection and after frontline therapy (e.g., trial designs used in GOG218 and ICON7 – details mentioned in Introduction). In this type of trial design,

women would be assigned to receive standard chemotherapy after surgical cytoreduction with and without the investigational agent during the therapy and with and without the agent after chemotherapy has ended for a pre-specified length of time.

Due to the activation of the PI3K/AKT pathway in angiogenesis and the resistant endothelial studies from this study, consideration could also be given to the addition of MSC2363318A to bevacizumab. The work presented here suggests that the addition of MSC2363318A to bevacizumab in the resistant setting may resensitize the tumor cells to therapy.

Due to the emergence of resistance to anti-angiogenesis therapy clinically, we are currently investigating whether MSC2363318A can overcome such resistance, and we are currently studying this in a model of adaptive resistance. This model requires intraperitoneal injections of luciferase-labeled cells to allow for confirmation of tumor establishment with bioluminescence imaging with randomization to two treatment groups: (1) control and (2) bevacizumab treatment. After three weeks of continuous bevacizumab treatment and weekly imaging, mice will be subsequently divided into bevacizumab-sensitive and bevacizumab-resistant groups based on tumor growth as evidenced by increased bioluminescence intensity in previously stable tumor burden. At the emergence of resistance in the previously sensitive group, MSC2363318A is added to the bevacizumab treatment. The combined treatment will continued until mice become moribund. We hypothesize that the additional of MSC2363318A at the emergence of resistance will halt tumor growth and prolong survival, as compared to either control or bevacizumab treatment alone.

As a follow-up to this preclinical study, we could identify women whose tumors "breakthrough" bevacizumab in the recurrent setting. Women could subsequently be randomized to receive continued bevacizumab with the addition of MSC2363318A or another standard therapy for recurrent disease by the National Comprehensive Cancer Network (NCCN) guidelines. Using more frequent imaging and markers of clinical response, progression free survival and overall survival of these two groups could be compared.

Other important niches to consider would be the effect of MSC2363318A on bulky tumors. This pre-clinical model is also currently being investigated after injection of luciferase-labeled uterine cells that were injected into the uterine horn. After established, measurable tumor growth is recorded by IVIS imaging, mice were randomized to four different treatment groups: (1) vehicle; (2) MSC2363318A; (3) paclitaxel; and (4) MSC2363318A and paclitaxel. Weekly quantifications of tumor volumes are made and mice are sacrificed with they become moribund. The effect of MSC2363318A as a monotherapy and in combination with chemotherapy on survival must be further investigated.

With the ever increasing number of targeted therapies, the addition of MSC2363318A with other novel agents should be tested. This includes poly-ADP ribose polymerase (PARP) inhibitors recently approved for recurrent ovarian cancer in *BRCA* mutation carriers. Preclinical work has shown that PI3K inhibition is correlated with the loss of homologous recombination repair, which increases DNA damage, and could lead to further sensitization of tumor cells by PARP inhibition [79]. An ongoing phase I trial combines olaparib, a PARP inhibitor, with a PI3K inhibitor in patients with

high grade serous ovarian cancer and triple negative breast cancer [80]. This combination has been already investigated in pre-clinical models of triple negative breast cancer. In this study, a pan-class IA PI3K inhibitor (NVP-BKM120) was combined with olaparib, which delayed tumor doubling in the combination therapy groups [79,81]. While olaparib is currently only approved for women with *BRCA* mutations, the addition of a PI3K/AKT inhibitor such as MSC2363318A could potentially make tumor cells without a somatic or germline *BRCA* mutation sensitive even more sensitive to PARP inhibition.

Study limitations

Here, we show compelling evidence that MSC2363318A promotes anti-tumoral growth and proliferation in pre-clinical models of ovarian and uterine cancer. High YAP1 expression is correlated with resistance to apoptosis after treatment with MSC2363318A. The mechanism of how YAP1 contributes to resistance remains unknown at this point. Profiling resistant cells such as SKOV3ip1, Ishikawa, and KLE after YAP1 knockdown and performing genomic profiles would give further insight into this mechanism. In cells that were transfected to overexpress YAP1, there was a slight protection against cell death, but this slight increase does not account for the protection afforded by nontransformed cells that overexpress YAP1.

Another limitation to this work is that only ovarian and uterine models were investigated. The PI3K/AKT pathway is one of the most frequently activated signaling pathways in cancer, so MSC2363318A may have broader effects on tumor growth in

other solid malignancies. Patient derived xenograft models should be considered in future studies.

Implications

On the basis and considerations described here, we show that MSC2363318A has therapeutic efficacy in multiple ovarian and uterine orthotopic models. Reductions in tumor weight, number of metastatic sites and nodules were observed without dose limiting side effects. This dual AKT1, AKT3, and P70S6K inhibitor inhibits cellular proliferation, promotes tumoral apoptosis, and decreases small vessel formation. The efficacy observed makes MSC2363318A a novel small molecule therapeutic that is worthy of further clinical development in patients in the frontline in combination with paclitaxel or in the recurrent setting. Our RPPA and *in vitro* validation suggest that YAP1 represents a biomarker that may identify those patients whose tumor may be most sensitive to this type of dual inhibition. Further, mechanistic studies are needed to better understand the molecular biology between these two pathways.

Moreover, given our findings *in vivo* and the effects of MSC2363318A on angiogenesis, we showed that in the resistant setting, the additional of MSC2363318A may allow for resensitization to anti-angiogenic agents. The addition of MSC2363318A to patients who have become resistant to bevacizumab may improve survival and prolonged, durable responses.

Conclusions:

Our preclinical data demonstrate that MSC2363318A may be therapeutically beneficial to ovarian and uterine cancer patients in combination with taxane-based therapies or anti-angiogenic therapies in the sensitive and resistant setting. YAP1 represents a potential predictive biomarker for predicting sensitivity of the cancer response to this treatment.

References

[1] A. Jemal, F. Bray, M.M. Center, J. Ferlay, E. Ward, D. Forman, Global cancer statistics, CA Cancer J Clin 61 (2011) 69-90.

[2] E. Banks, The epidemiology of ovarian cancer, Methods Mol Med 39 (2001) 3-11.

[3] A.P. Heintz, F. Odicino, P. Maisonneuve, U. Beller, J.L. Benedet, W.T. Creasman, H.Y. Ngan, M. Sideri, S. Pecorelli, Carcinoma of the ovary, J Epidemiol Biostat 6 (2001) 107-138.

[4] A.P. Heintz, F. Odicino, P. Maisonneuve, M.A. Quinn, J.L. Benedet, W.T. Creasman, H.Y. Ngan, S. Pecorelli, U. Beller, Carcinoma of the ovary. FIGO 26th Annual Report on the Results of Treatment in Gynecological Cancer, Int J Gynaecol Obstet 95 Suppl 1 (2006) S161-192.

[5] http://seer.cancer.gov/statfacts/html/corp.html. Accessed 15 May 2015.

[6] J.V. Bokhman, Two pathogenetic types of endometrial carcinoma, Gynecol Oncol 15 (1983) 10-17.

[7] A.S. Felix, J.L. Weissfeld, R.A. Stone, R. Bowser, M. Chivukula, R.P. Edwards, F. Linkov, Factors associated with Type I and Type II endometrial cancer, Cancer Causes Control 21 (2010) 1851-1856.

[8] J.L. Benedet, H. Bender, H. Jones, 3rd, H.Y. Ngan, S. Pecorelli, FIGO staging classifications and clinical practice guidelines in the management of gynecologic cancers. FIGO Committee on Gynecologic Oncology, Int J Gynaecol Obstet 70 (2000) 209-262.

[9] A.M. Nick, R.L. Coleman, P.T. Ramirez, A.K. Sood, A framework for a personalized surgical approach to ovarian cancer, Nat Rev Clin Oncol 12 (2015) 239-245.

[10] R.A. Burger, M.W. Sill, B.J. Monk, B.E. Greer, J.I. Sorosky, Phase II trial of bevacizumab in persistent or recurrent epithelial ovarian cancer or primary peritoneal cancer: a Gynecologic Oncology Group Study, J Clin Oncol 25 (2007) 5165-5171.

[11] A.A. Garcia, H. Hirte, G. Fleming, D. Yang, D.D. Tsao-Wei, L. Roman, S. Groshen, S. Swenson, F. Markland, D. Gandara, S. Scudder, R. Morgan, H. Chen, H.J. Lenz, A.M. Oza, Phase II clinical trial of bevacizumab and low-dose metronomic oral cyclophosphamide in recurrent ovarian cancer: a trial of the California, Chicago, and Princess Margaret Hospital phase II consortia, J Clin Oncol 26 (2008) 76-82.

[12] J. Ledermann, P. Harter, C. Gourley, M. Friedlander, I. Vergote, G. Rustin, C. Scott, W. Meier, R. Shapira-Frommer, T. Safra, D. Matei, E. Macpherson, C. Watkins, J. Carmichael, U. Matulonis, Olaparib maintenance therapy in platinum-sensitive relapsed ovarian cancer, N Engl J Med 366 (2012) 1382-1392.

[13] J. Ledermann, P. Harter, C. Gourley, M. Friedlander, I. Vergote, G. Rustin, C.L. Scott, W. Meier, R. Shapira-Frommer, T. Safra, D. Matei, A. Fielding, S. Spencer, B. Dougherty, M. Orr, D. Hodgson, J.C. Barrett, U. Matulonis, Olaparib maintenance therapy in patients with platinum-sensitive relapsed serous ovarian cancer: a preplanned retrospective analysis of outcomes by BRCA status in a randomised phase 2 trial, Lancet Oncol 15 (2014) 852-861.

[14] H. Gallion, W.A. Christopherson, R.L. Coleman, L. DeMars, T. Herzog, S. Hosford, H. Schellhas, A. Wells, B.U. Sevin, Progression-free interval in ovarian cancer and predictive value of an ex vivo chemoresponse assay, Int J Gynecol Cancer 16 (2006) 194-201.

[15] D.H. Kern, L.M. Weisenthal, Highly specific prediction of antineoplastic drug resistance with an in vitro assay using suprapharmacologic drug exposures, J Natl Cancer Inst 82 (1990) 582-588.

[16] R.A. Burger, M.F. Brady, M.A. Bookman, G.F. Fleming, B.J. Monk, H. Huang, R.S. Mannel, H.D. Homesley, J. Fowler, B.E. Greer, M. Boente, M.J. Birrer, S.X. Liang, G. Gynecologic Oncology, Incorporation of bevacizumab in the primary treatment of ovarian cancer, N Engl J Med 365 (2011) 2473-2483.

[17] T.J. Perren, A.M. Swart, J. Pfisterer, J.A. Ledermann, E. Pujade-Lauraine, G. Kristensen, M.S. Carey, P. Beale, A. Cervantes, C. Kurzeder, A. du Bois, J. Sehouli, R. Kimmig, A. Stahle, F. Collinson, S. Essapen, C. Gourley, A. Lortholary, F. Selle, M.R. Mirza, A. Leminen, M. Plante, D. Stark, W. Qian, M.K. Parmar, A.M. Oza, I. Investigators, A phase 3 trial of bevacizumab in ovarian cancer, N Engl J Med 365 (2011) 2484-2496.

[18] S.A. Cannistra, U.A. Matulonis, R.T. Penson, J. Hambleton, J. Dupont, H. Mackey, J. Douglas, R.A. Burger, D. Armstrong, R. Wenham, W. McGuire, Phase II study of bevacizumab in patients with platinum-resistant ovarian cancer or peritoneal serous cancer, J Clin Oncol 25 (2007) 5180-5186.

[19] S. Pecorelli, Revised FIGO staging for carcinoma of the vulva, cervix, and endometrium, Int J Gynaecol Obstet 105 (2009) 103-104.

[20] J.N. Barlin, I. Puri, R.E. Bristow, Cytoreductive surgery for advanced or recurrent endometrial cancer: a meta-analysis, Gynecol Oncol 118 (2010) 14-18.

[21] N. Cancer Genome Atlas Research, Integrated genomic analyses of ovarian carcinoma, Nature 474 (2011) 609-615.

[22] N. Cancer Genome Atlas Research, C. Kandoth, N. Schultz, A.D. Cherniack, R. Akbani, Y. Liu, H. Shen, A.G. Robertson, I. Pashtan, R. Shen, C.C. Benz, C. Yau, P.W. Laird, L. Ding, W. Zhang, G.B. Mills, R. Kucherlapati, E.R. Mardis, D.A. Levine, Integrated genomic characterization of endometrial carcinoma, Nature 497 (2013) 67-73.

[23] D.A. Fruman, C. Rommel, PI3K and cancer: lessons, challenges and opportunities, Nat Rev Drug Discov 13 (2014) 140-156.

[24] D. Hanahan, R.A. Weinberg, Hallmarks of cancer: the next generation, Cell 144 (2011) 646-674.

[25] C. Gewinner, Z.C. Wang, A. Richardson, J. Teruya-Feldstein, D. Etemadmoghadam, D. Bowtell, J. Barretina, W.M. Lin, L. Rameh, L. Salmena, P.P. Pandolfi, L.C. Cantley, Evidence that inositol polyphosphate 4-phosphatase type II is a tumor suppressor that inhibits PI3K signaling, Cancer Cell 16 (2009) 115-125.

[26] V. Zinzalla, D. Stracka, W. Oppliger, M.N. Hall, Activation of mTORC2 by association with the ribosome, Cell 144 (2011) 757-768.

[27] M. Laplante, D.M. Sabatini, mTOR signaling in growth control and disease, Cell 149 (2012) 274-293.

[28] K.D. Courtney, R.B. Corcoran, J.A. Engelman, The PI3K pathway as drug target in human cancer, J Clin Oncol 28 (2010) 1075-1083.

[29] Y. Samuels, K. Ericson, Oncogenic PI3K and its role in cancer, Curr Opin Oncol 18 (2006) 77-82.

[30] M.S. Song, L. Salmena, P.P. Pandolfi, The functions and regulation of the PTEN tumour suppressor, Nat Rev Mol Cell Biol 13 (2012) 283-296.

[31] K. Obata, S.J. Morland, R.H. Watson, A. Hitchcock, G. Chenevix-Trench, E.J. Thomas, I.G. Campbell, Frequent PTEN/MMAC mutations in endometrioid but not serous or mucinous epithelial ovarian tumors, Cancer Res 58 (1998) 2095-2097.

[32] H.J. Yang, V.W. Liu, Y. Wang, P.C. Tsang, H.Y. Ngan, Differential DNA methylation profiles in gynecological cancers and correlation with clinico-pathological data, BMC Cancer 6 (2006) 212.

[33] J.D. Carpten, A.L. Faber, C. Horn, G.P. Donoho, S.L. Briggs, C.M. Robbins, G. Hostetter, S. Boguslawski, T.Y. Moses, S. Savage, M. Uhlik, A. Lin, J. Du, Y.W. Qian, D.J. Zeckner, G. Tucker-Kellogg, J. Touchman, K. Patel, S. Mousses, M. Bittner, R.

Schevitz, M.H. Lai, K.L. Blanchard, J.E. Thomas, A transforming mutation in the pleckstrin homology domain of AKT1 in cancer, Nature 448 (2007) 439-444.

[34] J.Q. Cheng, A.K. Godwin, A. Bellacosa, T. Taguchi, T.F. Franke, T.C. Hamilton, P.N. Tsichlis, J.R. Testa, AKT2, a putative oncogene encoding a member of a subfamily of protein-serine/threonine kinases, is amplified in human ovarian carcinomas, Proc Natl Acad Sci U S A 89 (1992) 9267-9271.

[35] D.A. Levine, F. Bogomolniy, C.J. Yee, A. Lash, R.R. Barakat, P.I. Borgen, J. Boyd, Frequent mutation of the PIK3CA gene in ovarian and breast cancers, Clin Cancer Res 11 (2005) 2875-2878.

[36] A.J. Philp, I.G. Campbell, C. Leet, E. Vincan, S.P. Rockman, R.H. Whitehead, R.J. Thomas, W.A. Phillips, The phosphatidylinositol 3'-kinase p85alpha gene is an oncogene in human ovarian and colon tumors, Cancer Res 61 (2001) 7426-7429.

[37] M. Whitman, C.P. Downes, M. Keeler, T. Keller, L. Cantley, Type I phosphatidylinositol kinase makes a novel inositol phospholipid, phosphatidylinositol-3-phosphate, Nature 332 (1988) 644-646.

[38] M.E. Urick, M.L. Rudd, A.K. Godwin, D. Sgroi, M. Merino, D.W. Bell, PIK3R1 (p85alpha) is somatically mutated at high frequency in primary endometrial cancer, Cancer Res 71 (2011) 4061-4067.

[39] M.L. Rudd, J.C. Price, S. Fogoros, A.K. Godwin, D.C. Sgroi, M.J. Merino, D.W. Bell, A unique spectrum of somatic PIK3CA (p110alpha) mutations within primary endometrial carcinomas, Clin Cancer Res 17 (2011) 1331-1340.

[40] B. Weigelt, S. Banerjee, Molecular targets and targeted therapeutics in endometrial cancer, Curr Opin Oncol 24 (2012) 554-563.

[41] A.P. Myers, New strategies in endometrial cancer: targeting the PI3K/mTOR pathway--the devil is in the details, Clin Cancer Res 19 (2013) 5264-5274.

[42] P. Carmeliet, R.K. Jain, Molecular mechanisms and clinical applications of angiogenesis, Nature 473 (2011) 298-307.

[43] M.C. Schmid, J.A. Varner, Myeloid cell trafficking and tumor angiogenesis, Cancer Lett 250 (2007) 1-8.

[44] H. Zhong, K. Chiles, D. Feldser, E. Laughner, C. Hanrahan, M.M. Georgescu, J.W. Simons, G.L. Semenza, Modulation of hypoxia-inducible factor 1alpha expression by the epidermal growth factor/phosphatidylinositol 3-kinase/PTEN/AKT/FRAP pathway in human prostate cancer cells: implications for tumor angiogenesis and therapeutics, Cancer Res 60 (2000) 1541-1545.

[45] N.M. Mazure, E.Y. Chen, K.R. Laderoute, A.J. Giaccia, Induction of vascular endothelial growth factor by hypoxia is modulated by a phosphatidylinositol 3-kinase/Akt signaling pathway in Ha-ras-transformed cells through a hypoxia inducible factor-1 transcriptional element, Blood 90 (1997) 3322-3331.

[46] C. Xia, Q. Meng, Z. Cao, X. Shi, B.H. Jiang, Regulation of angiogenesis and tumor growth by p110 alpha and AKT1 via VEGF expression, J Cell Physiol 209 (2006) 56-66.

[47] D. Guo, Q. Jia, H.Y. Song, R.S. Warren, D.B. Donner, Vascular endothelial cell growth factor promotes tyrosine phosphorylation of mediators of signal transduction that contain SH2 domains. Association with endothelial cell proliferation, J Biol Chem 270 (1995) 6729-6733.

[48] H.P. Gerber, A. McMurtrey, J. Kowalski, M. Yan, B.A. Keyt, V. Dixit, N. Ferrara, Vascular endothelial growth factor regulates endothelial cell survival through the phosphatidylinositol 3'-kinase/Akt signal transduction pathway. Requirement for Flk-1/KDR activation, J Biol Chem 273 (1998) 30336-30343.

[49] H. Gille, J. Kowalski, L. Yu, H. Chen, M.T. Pisabarro, T. Davis-Smyth, N. Ferrara, A repressor sequence in the juxtamembrane domain of Flt-1 (VEGFR-1) constitutively

inhibits vascular endothelial growth factor-dependent phosphatidylinositol 3'-kinase activation and endothelial cell migration, EMBO J 19 (2000) 4064-4073.

[50] A. Papapetropoulos, D. Fulton, K. Mahboubi, R.G. Kalb, D.S. O'Connor, F. Li, D.C. Altieri, W.C. Sessa, Angiopoietin-1 inhibits endothelial cell apoptosis via the Akt/survivin pathway, J Biol Chem 275 (2000) 9102-9105.

[51] I. Kim, H.G. Kim, J.N. So, J.H. Kim, H.J. Kwak, G.Y. Koh, Angiopoietin-1 regulates endothelial cell survival through the phosphatidylinositol 3'-Kinase/Akt signal transduction pathway, Circ Res 86 (2000) 24-29.

[52] C. Hermann, B. Assmus, C. Urbich, A.M. Zeiher, S. Dimmeler, Insulin-mediated stimulation of protein kinase Akt: A potent survival signaling cascade for endothelial cells, Arterioscler Thromb Vasc Biol 20 (2000) 402-409.

[53] B.J. Michell, J.E. Griffiths, K.I. Mitchelhill, I. Rodriguez-Crespo, T. Tiganis, S. Bozinovski, P.R. de Montellano, B.E. Kemp, R.B. Pearson, The Akt kinase signals directly to endothelial nitric oxide synthase, Curr Biol 9 (1999) 845-848.

[54] H. Nakagami, R. Morishita, K. Yamamoto, Y. Taniyama, M. Aoki, K. Matsumoto, T. Nakamura, Y. Kaneda, M. Horiuchi, T. Ogihara, Mitogenic and antiapoptotic actions of hepatocyte growth factor through ERK, STAT3, and AKT in endothelial cells, Hypertension 37 (2001) 581-586.

[55] E. Schonherr, B. Levkau, L. Schaefer, H. Kresse, K. Walsh, Decorin-mediated signal transduction in endothelial cells. Involvement of Akt/protein kinase B in up-regulation of p21(WAF1/CIP1) but not p27(KIP1), J Biol Chem 276 (2001) 40687-40692.

[56] S. Dimmeler, B. Assmus, C. Hermann, J. Haendeler, A.M. Zeiher, Fluid shear stress stimulates phosphorylation of Akt in human endothelial cells: involvement in suppression of apoptosis, Circ Res 83 (1998) 334-341.

[57] T. Simoncini, A. Hafezi-Moghadam, D.P. Brazil, K. Ley, W.W. Chin, J.K. Liao, Interaction of oestrogen receptor with the regulatory subunit of phosphatidylinositol-3-OH kinase, Nature 407 (2000) 538-541.

[58] I. Shiojima, K. Walsh, Role of Akt signaling in vascular homeostasis and angiogenesis, Circ Res 90 (2002) 1243-1250.

[59] R. Rupaimoole, S.Y. Wu, S. Pradeep, C. Ivan, C.V. Pecot, K.M. Gharpure, A.S. Nagaraja, G.N. Armaiz-Pena, M. McGuire, B. Zand, H.J. Dalton, J. Filant, J.B. Miller, C. Lu, N.C. Sadaoui, L.S. Mangala, M. Taylor, T. van den Beucken, E. Koch, C. Rodriguez-Aguayo, L. Huang, M. Bar-Eli, B.G. Wouters, M. Radovich, M. Ivan, G.A. Calin, W. Zhang, G. Lopez-Berestein, A.K. Sood, Hypoxia-mediated downregulation of miRNA biogenesis promotes tumour progression, Nat Commun 5 (2014) 5202.

[60] http://www.mdanderson.org/education-and-research/resources-for-professionals/scientific-resources/core-facilities-and-services/functional-proteomics-rppa-core/education-and-references/index.html. Accessed 15 May 2015.

[61] S. Iadevaia, Y. Lu, F.C. Morales, G.B. Mills, P.T. Ram, Identification of optimal drug combinations targeting cellular networks: integrating phospho-proteomics and computational network analysis, Cancer Res 70 (2010) 6704-6714.

[62] R. Tibes, Y. Qiu, Y. Lu, B. Hennessy, M. Andreeff, G.B. Mills, S.M. Kornblau, Reverse phase protein array: validation of a novel proteomic technology and utility for analysis of primary leukemia specimens and hematopoietic stem cells, Mol Cancer Ther 5 (2006) 2512-2521.

[63] http://www.broadinstitute.org/ccle/home. Accessed 1 April 2015.

[64] R. Dienstmann, J. Rodon, V. Serra, J. Tabernero, Picking the point of inhibition: a comparative review of PI3K/AKT/mTOR pathway inhibitors, Mol Cancer Ther 13 (2014) 1021-1031.

[65] S. Lopez, C.L. Schwab, E. Cocco, S. Bellone, E. Bonazzoli, D.P. English, P.E. Schwartz, T. Rutherford, R. Angioli, A.D. Santin, Taselisib, a selective inhibitor of PIK3CA, is highly effective on PIK3CA-mutated and HER2/neu amplified uterine serous carcinoma in vitro and in vivo, Gynecol Oncol 135 (2014) 312-317.

[66] C.O. Ndubaku, T.P. Heffron, S.T. Staben, M. Baumgardner, N. Blaquiere, E. Bradley, R. Bull, S. Do, J. Dotson, D. Dudley, K.A. Edgar, L.S. Friedman, R. Goldsmith, R.A. Heald, A. Kolesnikov, L. Lee, C. Lewis, M. Nannini, J. Nonomiya, J. Pang, S. Price, W.W. Prior, L. Salphati, S. Sideris, J.J. Wallin, L. Wang, B. Wei, D. Sampath, A.G. Olivero, Discovery of 2-{3-[2-(1-isopropyl-3-methyl-1H-1,2-4-triazol-5-yl)-5,6-dihydrobenzo[f]imidazo[1 ,2-d][1,4]oxazepin-9-yl]-1H-pyrazol-1-yl}-2-methylpropanamide (GDC-0032): a beta-sparing phosphoinositide 3-kinase inhibitor with high unbound exposure and robust in vivo antitumor activity, J Med Chem 56 (2013) 4597-4610.

[67] B. Weigelt, P.H. Warne, M.B. Lambros, J.S. Reis-Filho, J. Downward, PI3K pathway dependencies in endometrioid endometrial cancer cell lines, Clin Cancer Res 19 (2013) 3533-3544.

[68] K. Balakrishnan, M. Peluso, M. Fu, N.Y. Rosin, J.A. Burger, W.G. Wierda, M.J. Keating, K. Faia, S. O'Brien, J.L. Kutok, V. Gandhi, The Phosphoinositide-3-Kinase (PI3K)-Delta and Gamma Inhibitor, IPI-145, Overcomes Signals from the PI3K/AKT/S6 Pathway and Promotes Apoptosis in CLL, Leukemia (2015).

[69] G.B. Park, D.Y. Hur, D. Kim, Combining CAL-101 with Celecoxib Enhances Apoptosis of EBV-transformed B-Cells Through MAPK-induced ER Stress, Anticancer Res 35 (2015) 2699-2708.

[70] M. Matsushima, E. Kikuchi, K. Matsumoto, S. Hattori, T. Takeda, T. Kosaka, A. Miyajima, M. Oya, Intravesical dual PI3K/mTOR complex 1/2 inhibitor NVP-BEZ235 therapy in an orthotopic bladder cancer model, Int J Oncol (2015).

[71] H. Wang, L. Zhang, X. Yang, Y. Jin, S. Pei, D. Zhang, H. Zhang, B. Zhou, Y. Zhang, D. Lin, PUMA mediates the combinational therapy of 5-FU and NVP-BEZ235 in colon cancer, Oncotarget (2015).

[72] H.B. Salvesen, I.S. Haldorsen, J. Trovik, Markers for individualised therapy in endometrial carcinoma, Lancet Oncol 13 (2012) e353-361.

[73] J. Tan, Q. Yu, Molecular mechanisms of tumor resistance to PI3K-mTOR-targeted therapy, Chin J Cancer 32 (2013) 376-379.

[74] D.D. Sarbassov, S.M. Ali, S. Sengupta, J.H. Sheen, P.P. Hsu, A.F. Bagley, A.L. Markhard, D.M. Sabatini, Prolonged rapamycin treatment inhibits mTORC2 assembly and Akt/PKB, Mol Cell 22 (2006) 159-168.

[75] J. Tan, P.L. Lee, Z. Li, X. Jiang, Y.C. Lim, S.C. Hooi, Q. Yu, B55beta-associated PP2A complex controls PDK1-directed myc signaling and modulates rapamycin sensitivity in colorectal cancer, Cancer Cell 18 (2010) 459-471.

[76] J.C. Bendell, J. Rodon, H.A. Burris, M. de Jonge, J. Verweij, D. Birle, D. Demanse, S.S. De Buck, Q.C. Ru, M. Peters, M. Goldbrunner, J. Baselga, Phase I, dose-escalation study of BKM120, an oral pan-Class I PI3K inhibitor, in patients with advanced solid tumors, J Clin Oncol 30 (2012) 282-290.

[77] J. Rodon, R. Dienstmann, V. Serra, J. Tabernero, Development of PI3K inhibitors: lessons learned from early clinical trials, Nat Rev Clin Oncol 10 (2013) 143-153.

[78] R. Dienstmann, I. Brana, J. Rodon, J. Tabernero, Toxicity as a biomarker of efficacy of molecular targeted therapies: focus on EGFR and VEGF inhibiting anticancer drugs, Oncologist 16 (2011) 1729-1740.

[79] Y.H. Ibrahim, C. Garcia-Garcia, V. Serra, L. He, K. Torres-Lockhart, A. Prat, P. Anton, P. Cozar, M. Guzman, J. Grueso, O. Rodriguez, M.T. Calvo, C. Aura, O. Diez, I.T. Rubio, J. Perez, J. Rodon, J. Cortes, L.W. Ellisen, M. Scaltriti, J. Baselga, PI3K inhibition

impairs BRCA1/2 expression and sensitizes BRCA-proficient triple-negative breast cancer to PARP inhibition, Cancer Discov 2 (2012) 1036-1047.

[80] S. Mabuchi, H. Kuroda, R. Takahashi, T. Sasano, The PI3K/AKT/mTOR pathway as a therapeutic target in ovarian cancer, Gynecol Oncol 137 (2015) 173-179.

[81] A. Juvekar, L.N. Burga, H. Hu, E.P. Lunsford, Y.H. Ibrahim, J. Balmana, A. Rajendran, A. Papa, K. Spencer, C.A. Lyssiotis, C. Nardella, P.P. Pandolfi, J. Baselga, R. Scully, J.M. Asara, L.C. Cantley, G.M. Wulf, Combining a PI3K inhibitor with a PARP inhibitor provides an effective therapy for BRCA1-related breast cancer, Cancer Discov 2 (2012) 1048-1063.

Vita

Rebecca was born in King William, Virginia on April 28th, 1983, the daughter of Steve and Ellen Previs. She was raised on her family's farm, Burnt Quarters in King William, Virginia. After graduating from King William High School, King William, Virginia, she enrolled in the University of Richmond, Richmond, Virginia. She received a Bachelor of Arts and Science degrees in chemistry and rhetoric/communication studies with minors in biology and women's studies 2005. She attended the University Of Virginia School of Medicine, Charlottesville, Virginia and graduated with a Doctor of Medicine in 2009. She entered the Obstetrics and Gynecology residency program at Duke University School of Medicine, Durham, North Carolina, completing her training in 2013. In July 2013, she began a fellowship in Gynecologic Oncology at the University of Texas M.D. Anderson Cancer Center. Her two year Master's program during this fellowship was mentored by Dr. Anil Sood and focused on ovarian cancer metabolomics and the role of novel therapeutics in ovarian and uterine carcinoma including MSC2363318A, OMP-59R5, and GSK2256908.

Permanent Address:

7676 Phoenix Dr., Apt 1106

Houston, TX 77030